

11176-H188-R0-00

PROJECT TECHNICAL REPORT
TASK E-9E

ANALYSIS OF THE SPURIOUS SPECTRAL COMPONENTS
APPEARING ABOUT THE S-BAND CARRIER

NAS 9-8166

9 MAY 1969

Prepared for
NATIONAL AERONAUTICS AND SPACE ADMINISTRATION
MANNED SPACECRAFT CENTER
HOUSTON, TEXAS

FACILITY FORM 802

N70-18708
(ACCESSION NUMBER)

82
(PAGES)

NASA:CR102172
(NASA CR OR TMX OR ALC NUMBER)

(THRU)

1
(CODE)

07
(CATEGORY)



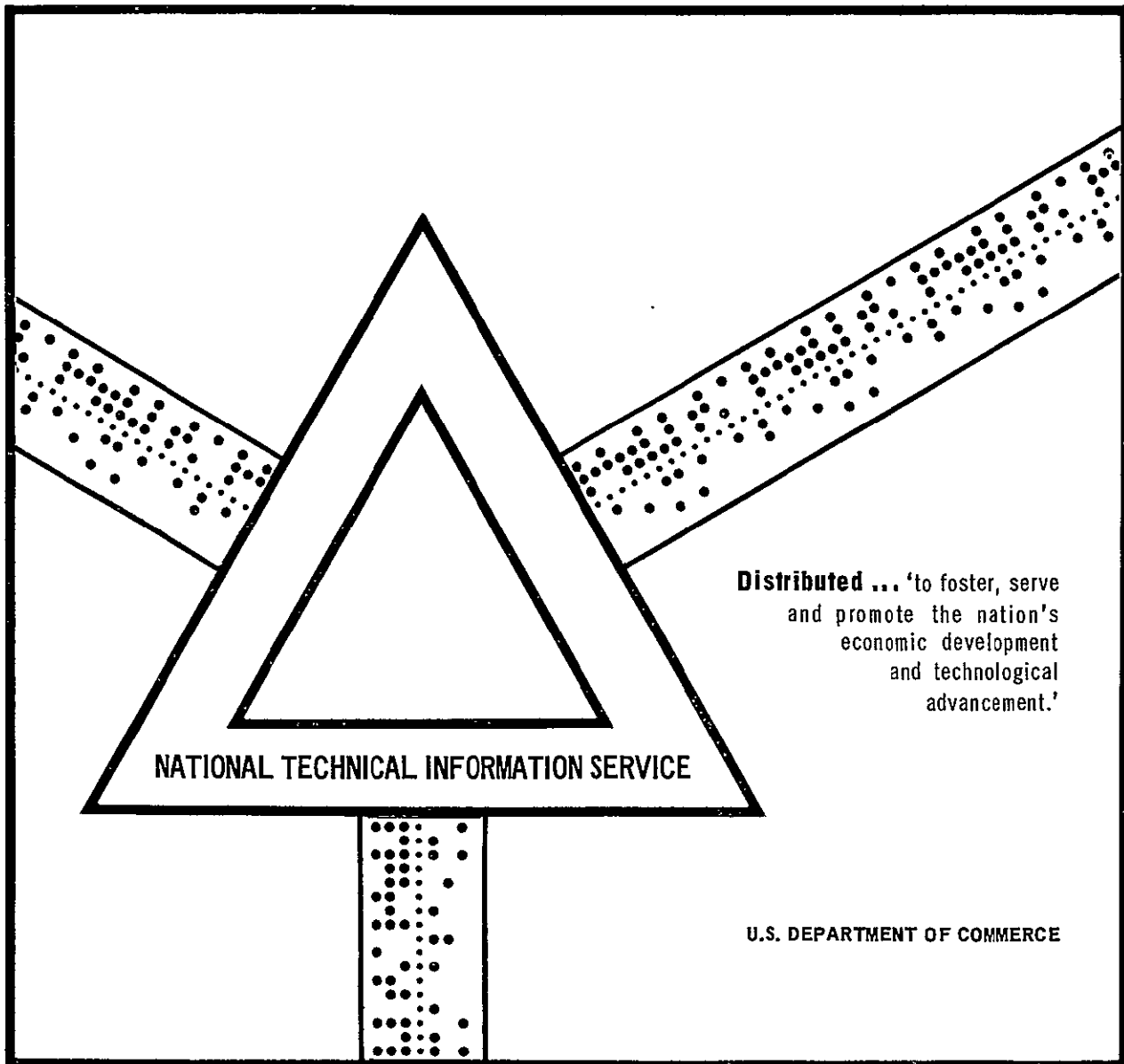
Reproduced by
NATIONAL TECHNICAL
INFORMATION SERVICE
Springfield, Va. 22151

N70 18708

ANALYSIS OF THE SPURIOUS SPECTRAL COMPONENTS
APPEARING ABOUT THE S-BAND CARRIER

Patrick J. Ready

9 May 1969



PROJECT TECHNICAL REPORT
TASK E-9E

ANALYSIS OF THE SPURIOUS SPECTRAL COMPONENTS
APPEARING ABOUT THE S-BAND CARRIER

NAS 9-8166

9 MAY 1969

Prepared for
NATIONAL AERONAUTICS AND SPACE ADMINISTRATION
MANNED SPACECRAFT CENTER
HOUSTON, TEXAS

Prepared by
Patrick J. Ready

Approved by *G. L. Christen*
G. L. Christen, Manager
Task E-9E

Approved by *Davis Bartholomew*
Davis Bartholomew
Head of Communications
Systems Section

Approved by *John DeVillier*
John DeVillier, Manager
Communication and Sensor
Systems Department

CONTENTS

	Page
1. INTRODUCTION	1-1
2. THE TM PM/PM MODULATION PROCESS	2-1
3. A BASIC EXAMPLE - THE SQUARE WAVE CASE	3-1
4. THE TM SPUR-TO-CARRIER POWER RATIO	4-1
4.1 The Bit Period - Bandwidth Product	4-1
4.2 The S/C Ratio as a Function of the BPB Product	4-2
4.3 The S/C Ratio as a Function of the TM Modulation Index	4-6
5. THE TM SPUR ENVELOPE FUNCTION	5-1
6. A PROPOSED SPUR REDUCTION TECHNIQUE	6-1
7. COMPUTER SIMULATION OF THE TM PM/PM MODULATION PROCESS	7-1
8. SUMMARY OF RESULTS	8-1

APPENDIXES

A	THE FOURIER TRANSFORM OF A SINUSOID PHASE MODULATED BY A TIME LIMITED, APERIODIC PCM-NRZ CODE	A-1
B	THE RELATIVE SPUR AMPLITUDES AS A FUNCTION OF SUBCARRIER FILTER BANDWIDTH, TM MODULATION INDEX, AND TM BIT RATE	B-1
C	AMPLITUDE DISTORTION IN THE BAND- LIMITED, BIPHASE MODULATED SUBCARRIER	C-1
D	THE APPROXIMATION OF $\cos [\beta g(t)]$	D-1
E	THE SPECTRAL DENSITY OF A SINUSOID PHASE MODULATED BY A TIME-LIMITED, APERIODIC PCM-NRZ CODE	E-1
F	S/C POWER RATIO TABLES	F-1

ILLUSTRATIONS

	Page
2-1 The Basic Telemetry Channel Block Diagram	2-2
4-1 Spur-to-Carrier Ratio (for the First Spur) versus Subcarrier Filter Bandwidth and Bit Period - Bandwidth Product for Various Values of TM Modulation Index	4-3
4-2 Spur-to-Carrier Ratio (for the Second Spur) versus Subcarrier Filter Bandwidth and Bit Period - Bandwidth Product for Various Values of TM Modulation Index	4-4
4-3 Spur-to-Carrier Ratio (for the Third Spur) versus Subcarrier Filter Bandwidth and Bit Period - Bandwidth Product for Various Values of TM Modulation Index	4-5
4-4 Spur-to-Carrier Ratio (for the First Spur) versus TM Modulation Index for Five Values of the Bit Period - Bandwidth Product	4-7
4-5 Spur-to-Carrier Ratio (for the Second Spur) versus TM Modulation Index for Five Values of the Bit Period - Bandwidth Product	4-8
5-1 Normalized Envelope Function versus Distance from the S-band Carrier for a Fixed Value of TM Bit Rate and Subcarrier Filter Bandwidth	5-2
5-2 Normalized Spur Envelope Function versus Distance from the S-band Carrier for Three Values of the Subcarrier Filter Bandwidth	5-4
5-3 Normalized Maximum Value of the Envelope Function versus TM Subcarrier Filter Bandwidth	5-5
6-1 Proposed Spur Reduction Technique	6-2
6-2 Spur Reduction versus Gain Ratio	6-4
6-3 Carrier Power Increase versus the TM Modulation Index for Two Values of the Amplifier Gain Ratio	6-5
7-1 Diagram of the Equations Used in the Computer Simulation of the TM PM/PM Process	7-2
7-2 Computer Generated Spectrum of the TM PM/PM Signal	7-3
8-1 Predicted and Actual S/C Ratios versus TM Modulation Index for $T\Omega = 24.6$	8-2

ILLUSTRATIONS (Continued)

	Page	
A-1	m(t) versus Time	A-1
A-2	Real Part of $F(\omega, \alpha_n)$ versus Frequency ($f_0 = 1.024$ MHz) . .	A-6
A-3	Imaginary Part of $F(\omega, \alpha_n)$ versus Frequency ($f_0 = 1.024$ MHz)	A-7
B-1	The Cosine Integral	B-12
B-2	$T_1(\omega)$ versus Frequency.	B-14
C-1	Modulating Function Expressed as the Sum of a Series of Step Functions	C-1
C-2	Basic Step Function	C-3
C-3	Filtered Step Function (Equation (C-8))	C-4
C-4	Filtered Time Function Resulting from a Bit change	C-4
D-1	Cos(X) and Its Approximation for Values of X Less Than or Equal to 1.5	D-3

1. INTRODUCTION

Tests conducted at NASA/MSC on CSM S-band downlink carrier acquisition have shown that undesirable spectral components appear about the S-band carrier when the 1.024 MHz subcarrier is phase modulated with 51.2 kbps telemetry. The spurious spectral components, or spurs, were found on either side of the S-band carrier at integral multiples of the telemetry (TM) bit rate. The largest amplitude spurs were located at distances of ± 51.2 kHz and ± 102.4 kHz away from the S-band carrier (2106.4 MHz), both measured at -29 dB relative to the carrier.

As a result of the spurs, false carrier locks (lock on a spur rather than the carrier) had occurred on Manned Space Flight Network (MSFN) receivers using a sweep width of ± 90 kHz. It was found that a reduction of the sweep width to ± 37 kHz would prevent false acquisitions, since the first spur would not be located within the sweep range. However, a reduction in the sweep width could cause acquisition problems if the received carrier frequency was shifted more than ± 37 kHz due to doppler effects. (Doppler shifts of up to ± 55 kHz have been experienced on previous Apollo missions.)

The purposes of this study are

- a) To determine the cause of the spurs
- b) To determine when they will be present
- c) To relate the amplitude of the spurs to the TM modulation index, the subcarrier filter bandwidth, and the TM bit rate.
- d) To suggest methods to reduce or eliminate the spurs

In order to accomplish these four objectives, a mathematical analysis of the LM and CSM PM/PM TM modulation process has been completed. The resulting equations describe the spurs and are used to predict their location and magnitude. The equations also provide the needed relationships to determine the relative merits of various combinations of modulation index and subcarrier filter bandwidth.

Simulation of the TM modulation process was also performed on the SRU-1108 digital computer. The results are presented in this study and are compared with the theoretical predictions:

The assumptions made in this study are

- a) The TM subcarrier modulation index is less than 1.5.
- b) The subcarrier biphase modulator is perfectly balanced (symmetrical bit wave forms).
- c) The subcarrier band-pass filter is an ideal filter having constant gain and linear phase-shift over the passband.
- d) The S-band carrier frequency is greater than the TM subcarrier frequency.

2. THE TM PM/PM MODULATION PROCESS

It is assumed in this study that the basic TM modulation process used on the LM and CSM is that shown in Figure 2-1. Additional operations on the signal may or may not influence the location and/or amplitude of the spurs. Figure 2-1 represents the basic spur generating system.

The output of the biphase modulator is

$$f(t) = \sin [\omega_o t + m(t) \pi] \quad (2-1)$$

where ω_o is the subcarrier radian frequency, and $m(t)$ is related to the PCM-NRZ data by

$$m(t) = \begin{cases} 1, & \text{if the PCM-NRZ data} = + E \text{ volts} \\ 0, & \text{if the PCM-NRZ data} = 0 \text{ volts} \end{cases} \quad (2-2)$$

The band-pass filter shown in Figure 2-1 is assumed to have constant gain and linear phase-shift over the passband. The output of the filter will, as is shown in Appendix C, contain amplitude distortion.

The last step in the TM modulation process is the phase modulation of the S-band carrier by the filtered, biphase modulated subcarrier. The output of the PM mixer is

$$e(t) = A \sin [\omega_c t + \beta g(t)] \quad (2-3)$$

where β is the TM modulation index, ω_c is the S-band carrier radian frequency, and $g(t)$ is the filtered, biphase modulated subcarrier.

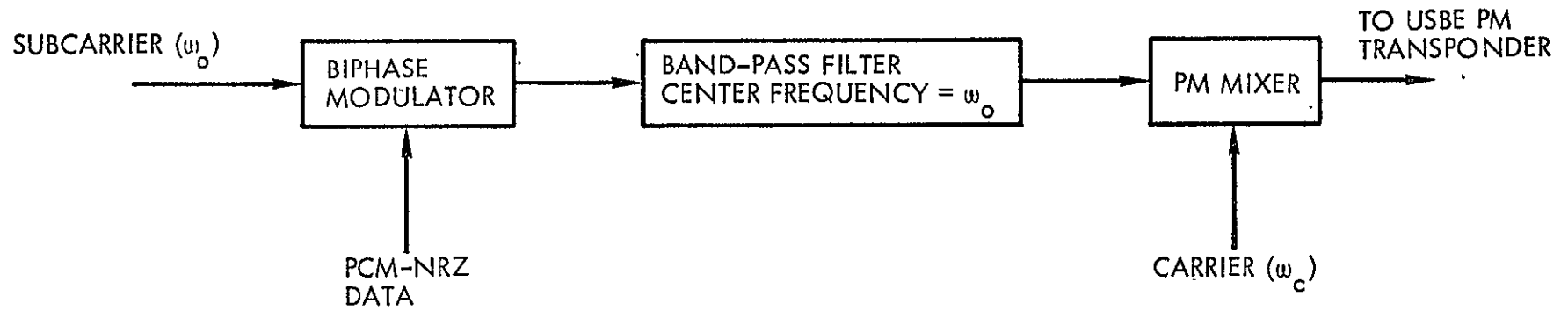


Figure 2-1. The Basic Telemetry Channel Block Diagram

3. A BASIC EXAMPLE - THE SQUARE WAVE CASE

An intuitive understanding of the spur generating process may be gained by making the simplifying assumption that $m(t)$ in Equation (2-2) is a sequence of alternating 1's and 0's (a square wave with period $2T$). With that assumption, $f(t)$ in Equation (2-1) becomes

$$f(t) = \pm \sin (\omega_o t) \quad (3-1)$$

$$f(t) = \frac{4}{\pi} \sin (\omega_o t) \sum_{n=1,3,\dots}^{\infty} \frac{1}{n} \sin \left(\frac{n\pi}{T} t \right) \quad (3-2)$$

If the subcarrier band-pass filter is assumed (for this example) to have bandwidth Ω , where

$$\frac{\pi}{T} < \Omega < \frac{3\pi}{T} \quad (3-3)$$

then the output of the filter will be

$$g(t) = \frac{4}{\pi} \sin (\omega_o t) \sin \left(\frac{\pi}{T} t \right) \quad (3-4)$$

and the output of the PM mixer will be

$$e(t) = A \sin \left[\omega_c t + \beta g(t) \right] \quad (3-5)$$

$$= A \sin \left[\omega_c t + \frac{4\beta}{\pi} \sin (\omega_o t) \sin \left(\frac{\pi}{T} t \right) \right] \quad (3-6)$$

$$= A \sin (\omega_c t) \cos \left[\frac{4\beta}{\pi} \sin (\omega_o t) \sin \left(\frac{\pi}{T} t \right) \right] \\ + A \cos (\omega_c t) \sin [\beta g(t)] \quad (3-7)$$

If $\beta g(t)$ is less than 1.5, then

$$e(t) \approx A \sin(\omega_c t) \left[1 - \frac{16a\beta^2}{\pi^2} \sin^2(\omega_o t) \sin^2\left(\frac{\pi}{T} t\right) \right] \\ + A \cos(\omega_c t) \sin[\beta g(t)] \quad (3-8)$$

where, as is shown in Appendix D

$$a = 0.4368 \quad (3-9)$$

A further expansion of Equation (3-8) gives

$$e(t) = A \left(1 - \frac{4a\beta^2}{\pi^2} \right) \sin(\omega_c t) + \frac{2Aa\beta^2}{\pi^2} \sin \left[\left(\omega_c \pm \frac{2\pi}{T} \right) t \right] \\ - \frac{Aa\beta^2}{\pi^2} \sin \left[\left(\omega_c \pm 2\omega_o \pm \frac{2\pi}{T} \right) t \right] + \frac{2Aa\beta^2}{\pi^2} \sin \left[\left(\omega_c \pm 2\omega_o \right) t \right] \\ + A \cos(\omega_c t) \sin[\beta g(t)] \quad (3-10)$$

It is evident from the second term in Equation (3-10) that the spectrum of $e(t)$ will contain a component (spur) at $\omega_c \pm \frac{2\pi}{T}$. The power of that component relative to the carrier is

$$R_{dB} = 20 \log_{10} \left\{ \frac{2a\beta^2}{\pi^2 - 4a\beta^2} \right\} \quad (3-11)$$

$$= -13.4 \text{ dB } (\beta = 1.3) \quad (3-12)$$

It was assumed for this example that the subcarrier band-pass filter allowed only the fundamental of the square wave to pass. As a result, only one set $(\omega_c \pm \frac{2\pi}{T})$ of spurs were generated. A bandwidth of

$$\frac{3\pi}{T} < \Omega < \frac{5\pi}{T} \quad (3-13)$$

would have generated spurs at $\omega_c \pm \frac{2\pi}{T}$, $\omega_c \pm \frac{4\pi}{T}$, and $\omega_c \pm \frac{6\pi}{T}$. That is, spurs in the downlink signal spectrum would be located at distances of one, two, and three times the TM bit rate away from the S-band carrier.

The assumption that $m(t)$ in Equation (2-2) is a square wave is not a realistic model of actual telemetry. The square wave case only serves as basic (worst case) example of how TM spurs might be generated. The more complex problem of random "1" and "0" bits is the subject of the rest of this report.

4. THE TM SPUR-TO-CARRIER POWER RATIO

As discussed in Section 3, the assumption of square wave telemetry does not give a realistic model of the TM PM/PM modulation process. The results of the analysis carried out in Appendix B for random telemetry are presented in this section. The discussion begins with a definition.

4.1 THE BIT PERIOD - BANDWIDTH PRODUCT

An important quantity encountered in the analysis and description of the TM spurs is the bit period - bandwidth (BPB) product.

$$\text{BPB product} = T\Omega \quad (4-1)$$

where T is the period of one TM bit (in seconds) and Ω is the TM subcarrier filter bandwidth (in radians per second). Typical values of the BPB product with present NASA parameters would be from 16 to 25.

The importance of the BPB product is brought out by an examination of the spur-to-carrier (S/C) power ratio derived in Appendix B and rewritten in Equation (4-2).

$$R_{dB}(k, \Omega, \beta, T) = 20 \log_{10} \left[\frac{-a}{2k} \left(\frac{\beta}{\pi} \right)^2 \frac{\left[\ln \left(\left| 2\pi k - \frac{T\Omega}{2} \right| \right) - C_i \left(\left| 2\pi k - \frac{T\Omega}{2} \right| \right) - \ln \left(\frac{T\Omega}{2} \right) + C_i \left(\frac{T\Omega}{2} \right) \right]}{1 - \frac{a\beta^2}{\pi} \left[S_i \left(\frac{T\Omega}{2} \right) - \frac{2}{T\Omega} \left(1 - \cos \left(\frac{T\Omega}{2} \right) \right) \right]} \right] \quad (4-2)$$

where β is the TM modulation index, and k is the spur index (k = 1 indicates the first spur either side of the S-band carrier, k = 2 indicates the second spur either side of the S-band carrier, etc.). The constant a is derived in Appendix D (a = 0.4368). The functions $C_1(x)$ and $S_1(x)$ refer to the cosine and sine integrals, respectively. Both $C_1(x)$ and $S_1(x)$ are well tabulated, and a plot of $C_1(x)$ is included in Appendix B.

The functional relationship expressed in Equation (4-2) may be used to predict the power (in dB) of the kth spur relative to the S-band carrier for a given combination of TM modulation index, subcarrier filter bandwidth, and TM bit rate. Equation (4-2) is basic to the results of this report.

4.2 THE S/C RATIO AS A FUNCTION OF THE BPB PRODUCT

Examination of Equation (4-2) shows that neither the bit period T nor the filter bandwidth Ω ever appear separately. Rather, they always appear together as the BPB product. This indicates that the effects of an increase (decrease) in the TM bit rate on the S/C ratio cannot be distinguished from a corresponding decrease (increase) of the subcarrier filter bandwidth. Or, stated another way, the effects on the S/C ratio resulting from a decrease (increase) in the bit rate may be completely negated by a corresponding decrease (increase) in the subcarrier filter bandwidth.

Figures 4-1, 4-2, and 4-3 are plots of the S/C ratio (Equation (4-2)) as a function of both the subcarrier filter bandwidth Ω (fixed T) and the BPB product. In all three figures the TM modulation index β appears as a parameter. It can be seen that the S/C ratio is maximum near $T\Omega = 4\pi k$ ($T\Omega = 12.6$ for the first spur, $T\Omega = 25.1$ for the second spur, etc.). The maximum value of the S/C ratio near $T\Omega = 4\pi k$ depends on the modulation index β , but a representative value for the first spur might be -19 dB with $\beta = 1.2$. The S/C ratio falls off rapidly for values of the BPB product less than $4\pi k$, and is (theoretically) infinitely small when the BPB product is less than $2\pi k$. A BPB product less than 2π ($k=1$) means that either the subcarrier filter bandwidth is less than the bit rate or that the bit rate is greater than the bandwidth. Whichever case is true, there will be no TM spurs. A BPB product less than 4π ($k=2$) means that the second spur will be very small. Similar statements are true for higher values of the spur index k .

As an example of how the family of curves in Figures 4-1, 4-2, and 4-3 could be used to predict S/C ratios, the following values are arbitrarily chosen: (1) $\beta = 1.2$ and (2) $T\Omega = 25.4$. From Figure 4-1 the first spur would be -30 dB relative to the carrier, the second spur (Figure 4-2) would be -23 dB, and the third spur (Figure 4-3) would be -40 dB. An increase in the BPB product to 29.3 would cause a 1 dB and a 3 dB reduction in the first two spurs, respectively, and a 4 dB increase in the third spur.

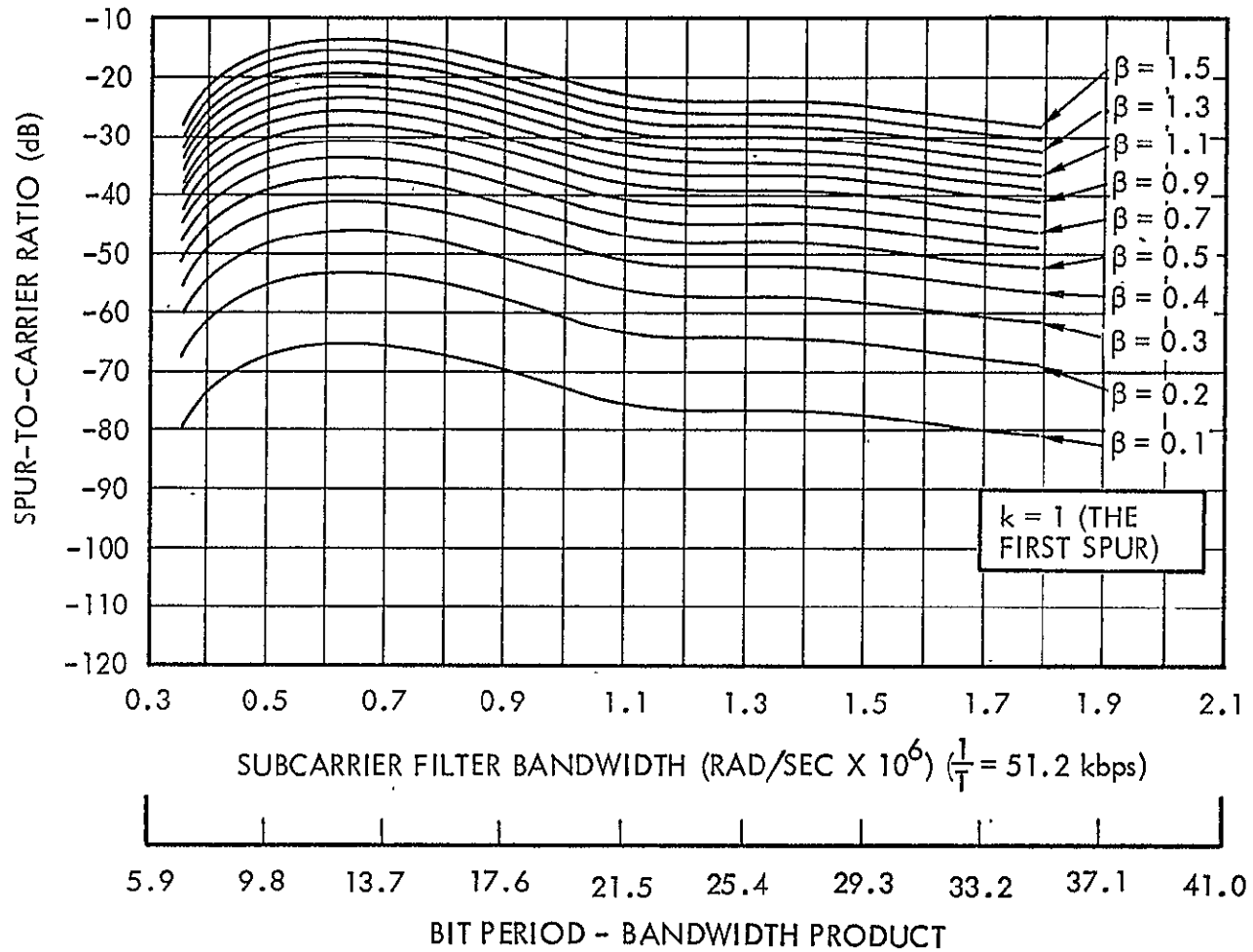


Figure 4-1. Spur-to-Carrier Ratio (for the First Spur) versus Subcarrier Filter Bandwidth and Bit Period - Bandwidth Product for Various Values of TM Modulation Index

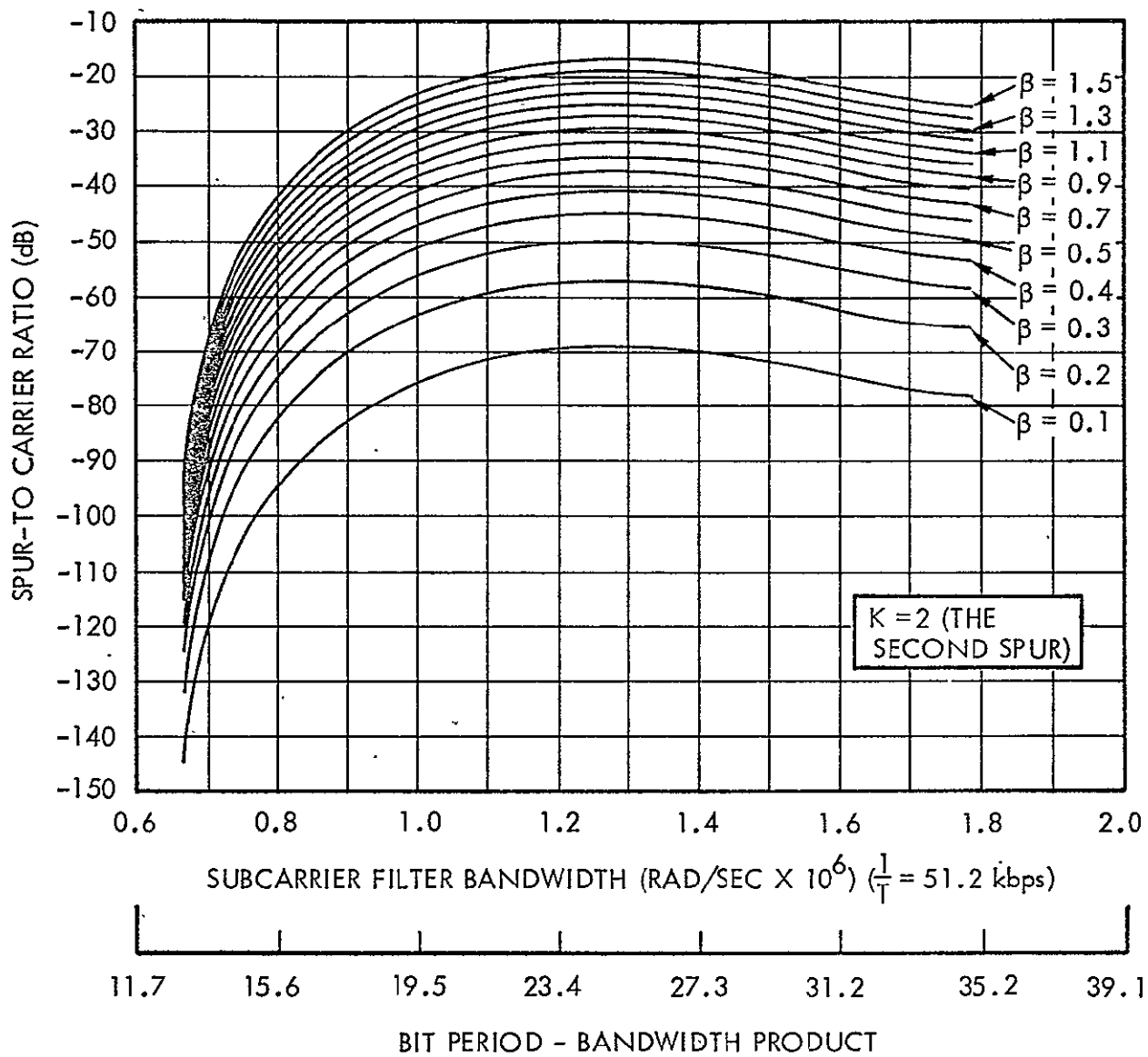


Figure 4-2. Spur-to-Carrier Ratio (for the Second Spur) versus Subcarrier Filter Bandwidth and Bit Period - Bandwidth Product for Various Values of TM Modulation Index

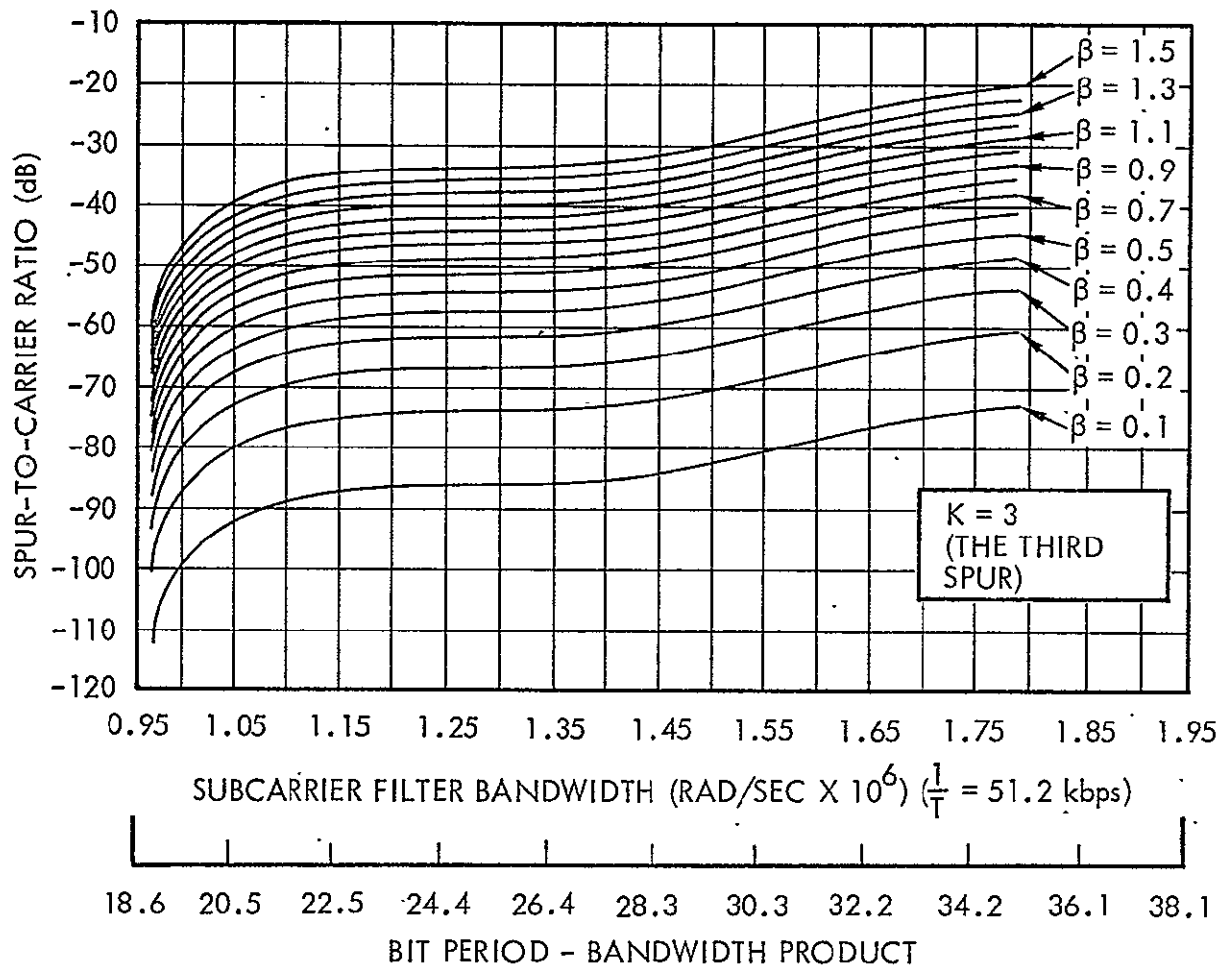


Figure 4-3. Spur-to-Carrier Ratio (for the Third Spur) versus Subcarrier Filter Bandwidth and Bit Period - Bandwidth Product for Various Values of TM Modulation Index

4.3 THE S/C RATIO AS A FUNCTION OF THE TM MODULATION INDEX

It is well known in the study of PM signals that an increase in the modulation index (up to $\beta = 2.4$ for sinusoidal modulation) will cause a reduction in the carrier power and an increase in the power found in the sidebands. A similar effect has been shown (in Appendix B) to occur with the TM spurs. As shown in Figures 4-4 and 4-5, an increase in the modulation index β causes an increase in the S/C ratio. (In both figures the BPB product appears as a parameter.) Figures 4-4 and 4-5 show that there is almost a linear relationship between the S/C ratio and the modulation index for values of β between 0.5 and 1.5. For values of β less than 0.5 there is a rapid decrease in the S/C ratio. It should be noted that for a given modulation index, an increase in the BPB product causes a downward shift in the curves in Figure 4-4, while the opposite is true in Figure 4-5. This effect was discussed in Section 4.2 when it was found that the S/C ratio peaked near $T\Omega = 4\pi k$. From Figure 4-4 it can be seen that an increase in the modulation index from 1.0 to 1.3 would cause an approximate 6 dB increase in the S/C ratio regardless of the BPB product. Similar results for the second spur may be determined from Figure 4-5.

The combined effects of the BPB product and the TM modulation index are presented in matrix form in Appendix F.

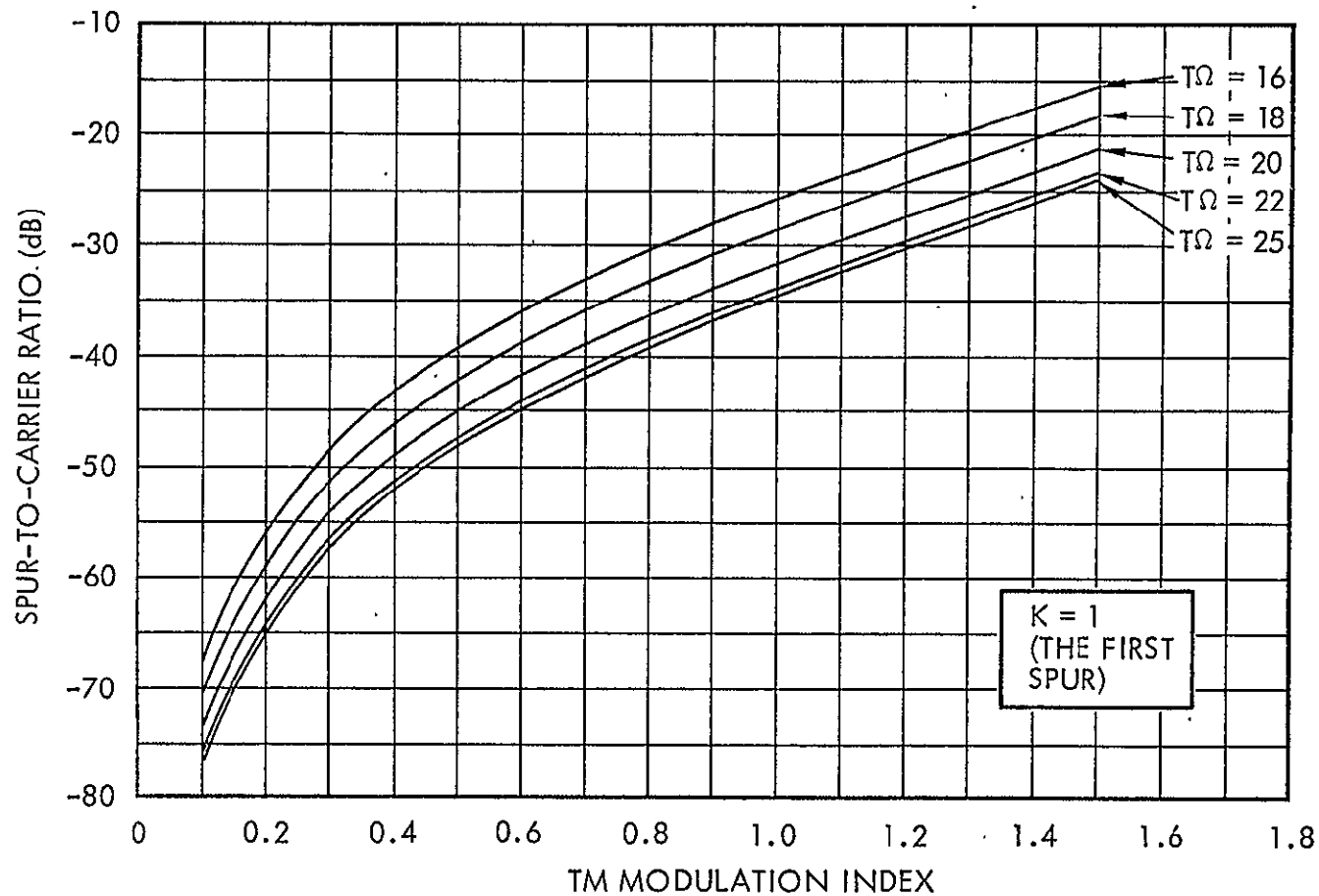


Figure 4-4. Spur-to-Carrier Ratio (for the First Spur) versus TM Modulation Index for Five Values of the Bit Period - Bandwidth Product

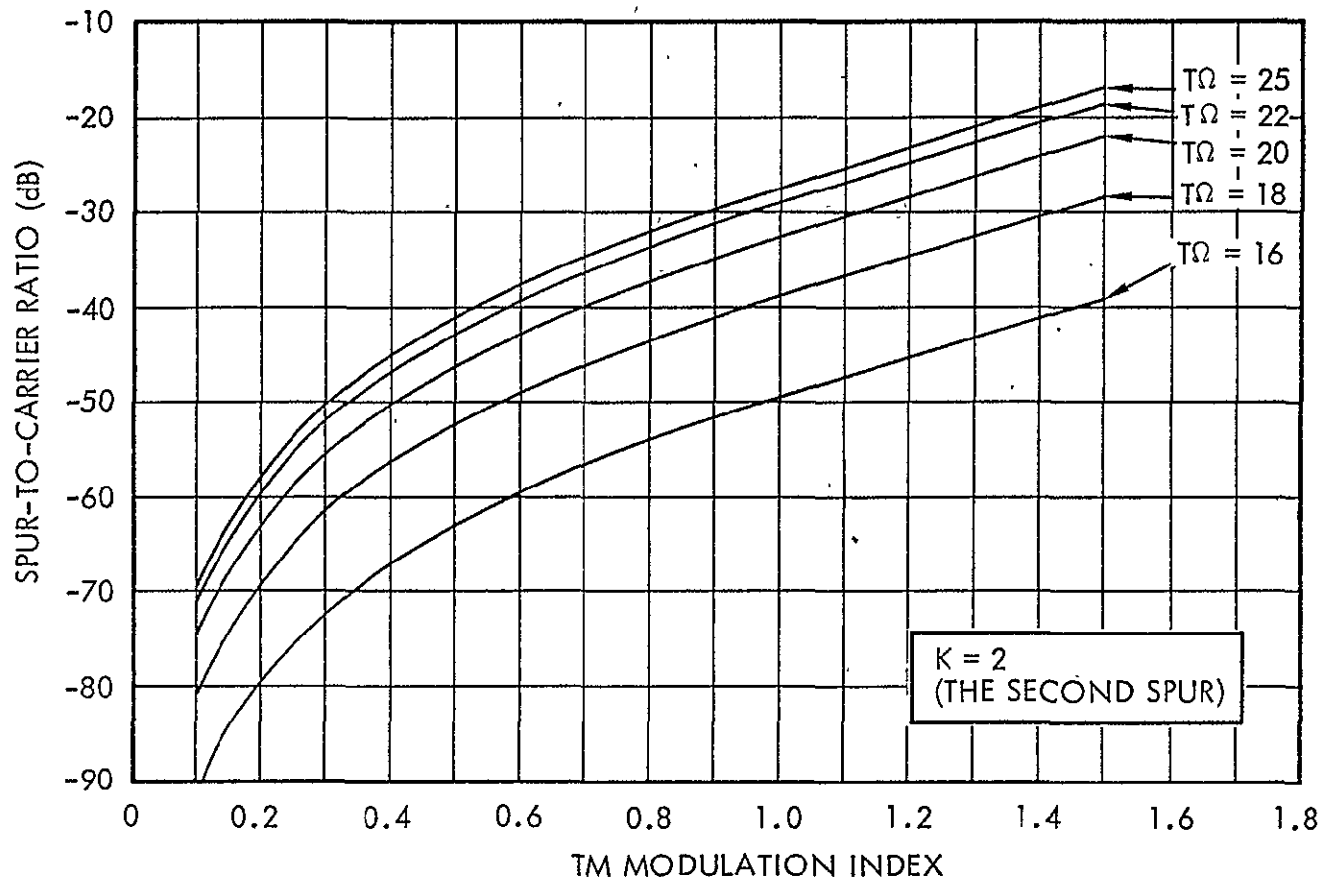


Figure 4-5. Spur-to-Carrier Ratio (for the Second Spur) versus TM Modulation Index for Five Values of the Bit Period - Bandwidth Product

5. THE TM SPUR ENVELOPE FUNCTION

Previous sections have discussed the power in the TM spurs relative to the S-band carrier as given by the S/C ratio. In those sections it was found that the S/C ratio was a function of the spur index k ($k = 1$ indicates the first spur either side of the S-band carrier, $k = 2$ indicates the second spur . . . etc). In other words, for a given modulation index and BPB product the first spur was not (in general) equal to the second spur, nor to the third spur, etc. In this section a discussion of the spurs relative to each other will be given.

It is shown in Appendix B that the "envelope function" describing the distribution of power in the spurs is given by

$$E(\omega_d) = \left\{ \frac{1}{\omega_d} \left[\ln \left(T \left| \omega_d - \frac{\Omega}{2} \right| \right) - C_i \left(T \left| \omega_d - \frac{\Omega}{2} \right| \right) - \ln \left(\frac{T\Omega}{2} \right) + C_i \left(\frac{T\Omega}{2} \right) \right] \right\}^2$$

where $1/T$ is the TM bit rate, Ω is the subcarrier filter bandwidth, ω_d is the distance (in radians per second) away from the S-band carrier, and $C_i(X)$ is the cosine integral described in Appendix B.

The power in a given spur relative to that of another spur is found by evaluating $E(\omega_d)$ at the location of each spur and taking $10 \log_{10}$ of the resulting ratio. For example, Figure 5-1 is a normalized plot of Equation (5-1) for a specific value of T and Ω . From the curve it can be determined that the normalized envelope function is approximately 0.175 at the first spur, and approximately 0.456 at the second spur. The ratio of the first to the second is 0.258, and

$$10 \log_{10} (0.258) = -5.88 \text{ dB} \tag{5-2}$$

Thus, the first spur is -5.88 dB below the second spur regardless of their power relative to the carrier. That is, if the second spur was -30 dB relative to the carrier, the first spur would be -30 dB - 5.88 dB, or -30 + (-5.88), or -35.88 dB relative to the carrier (for the specific values of T and Ω chosen).

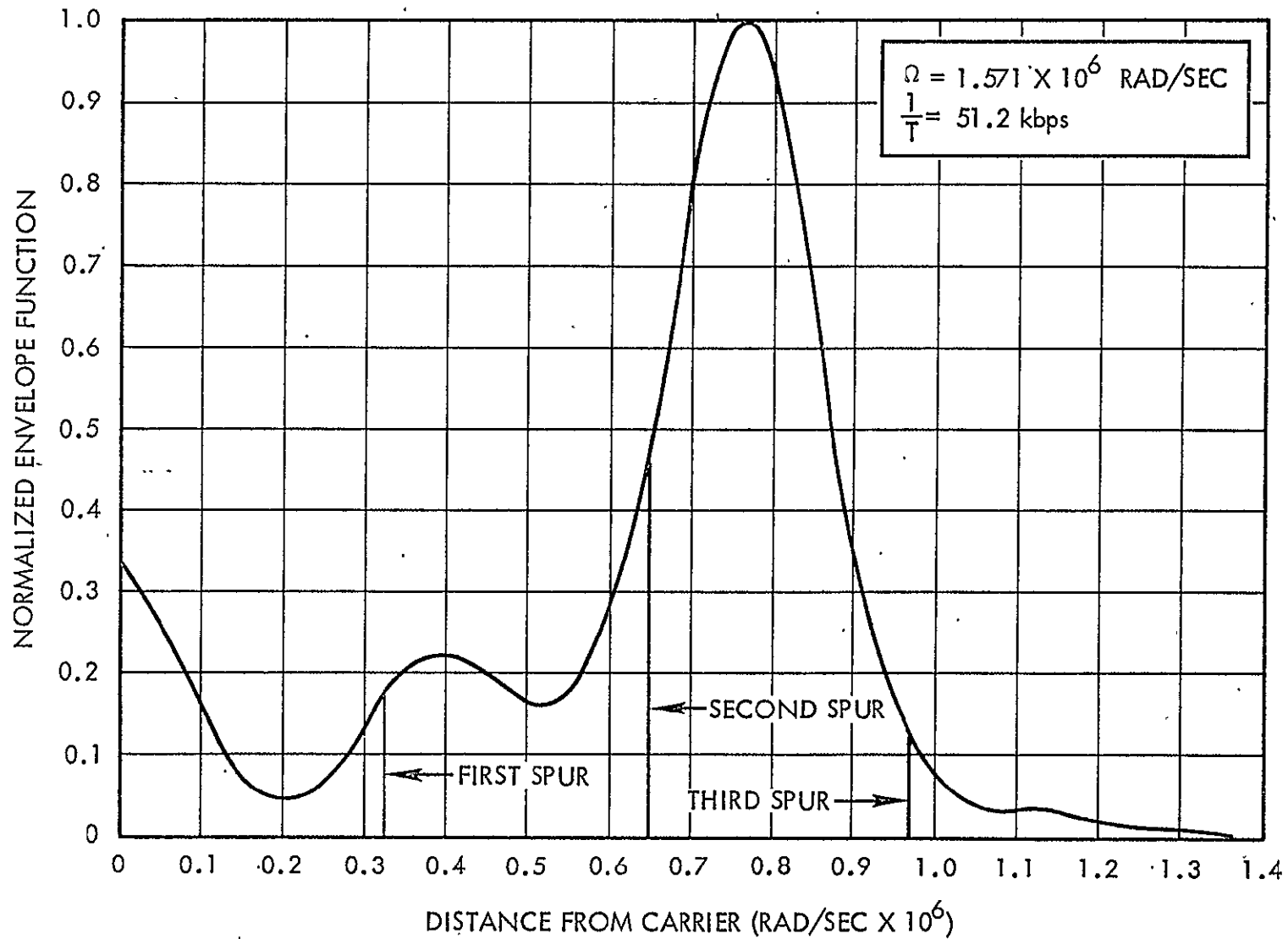


Figure 5-1. Normalized Envelope Function versus Distance from the S-band Carrier for a Fixed Value of TM Bit Rate and Subcarrier Filter Bandwidth

A family of curves is presented in Figure 5-2 with the subcarrier filter bandwidth as a parameter. It can be seen that an increase in Ω causes a general reduction in the envelope function.

Figure 5-3 is a plot of the normalized maximum value of the envelope function (for a specific bitrate) as a function of the subcarrier filter bandwidth. The figure is included to demonstrate the fact that the envelope function approaches zero as Ω becomes very small or very large.

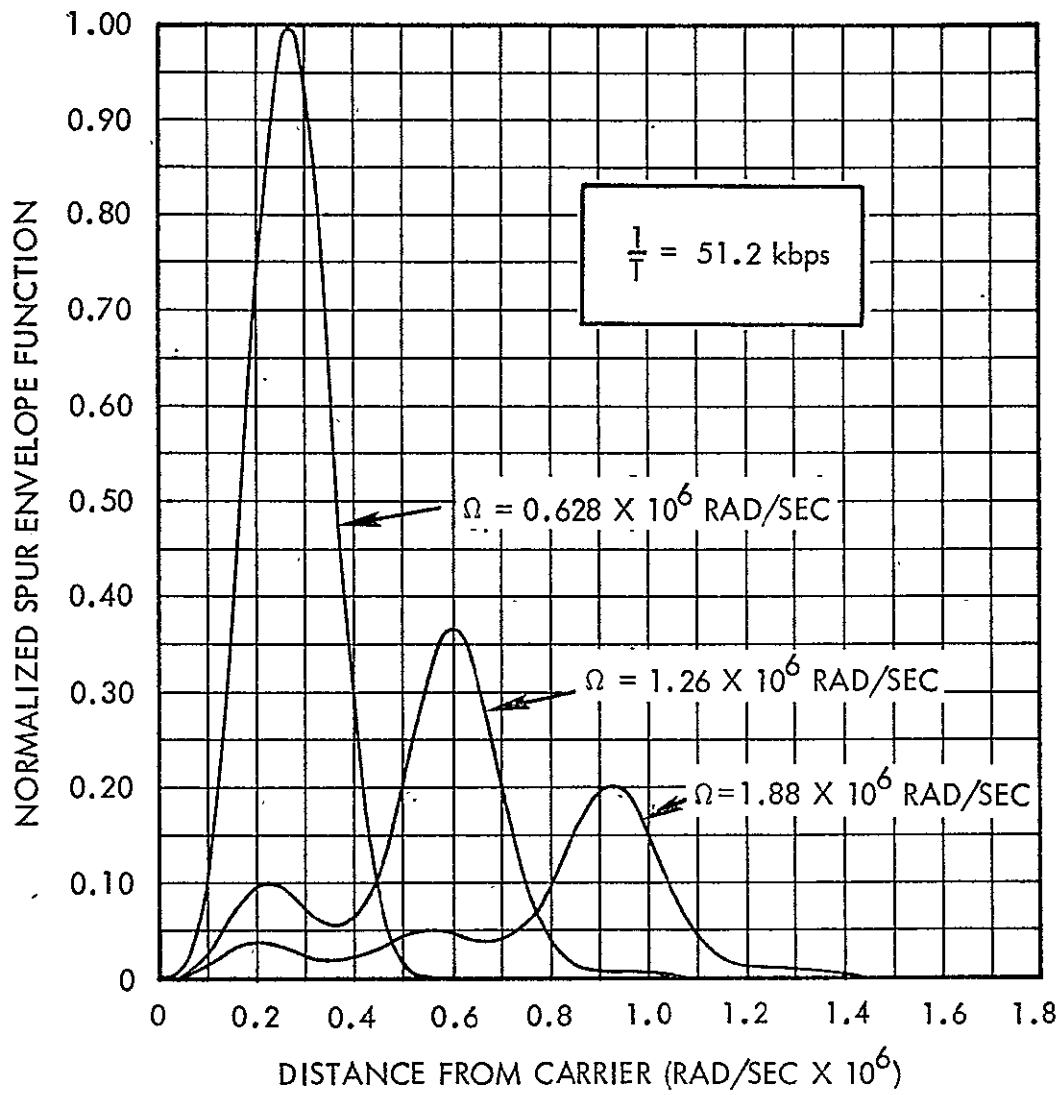


Figure 5-2. Normalized Spur Envelope Function versus Distance from the S-band Carrier for Three Values of the Subcarrier Filter Bandwidth

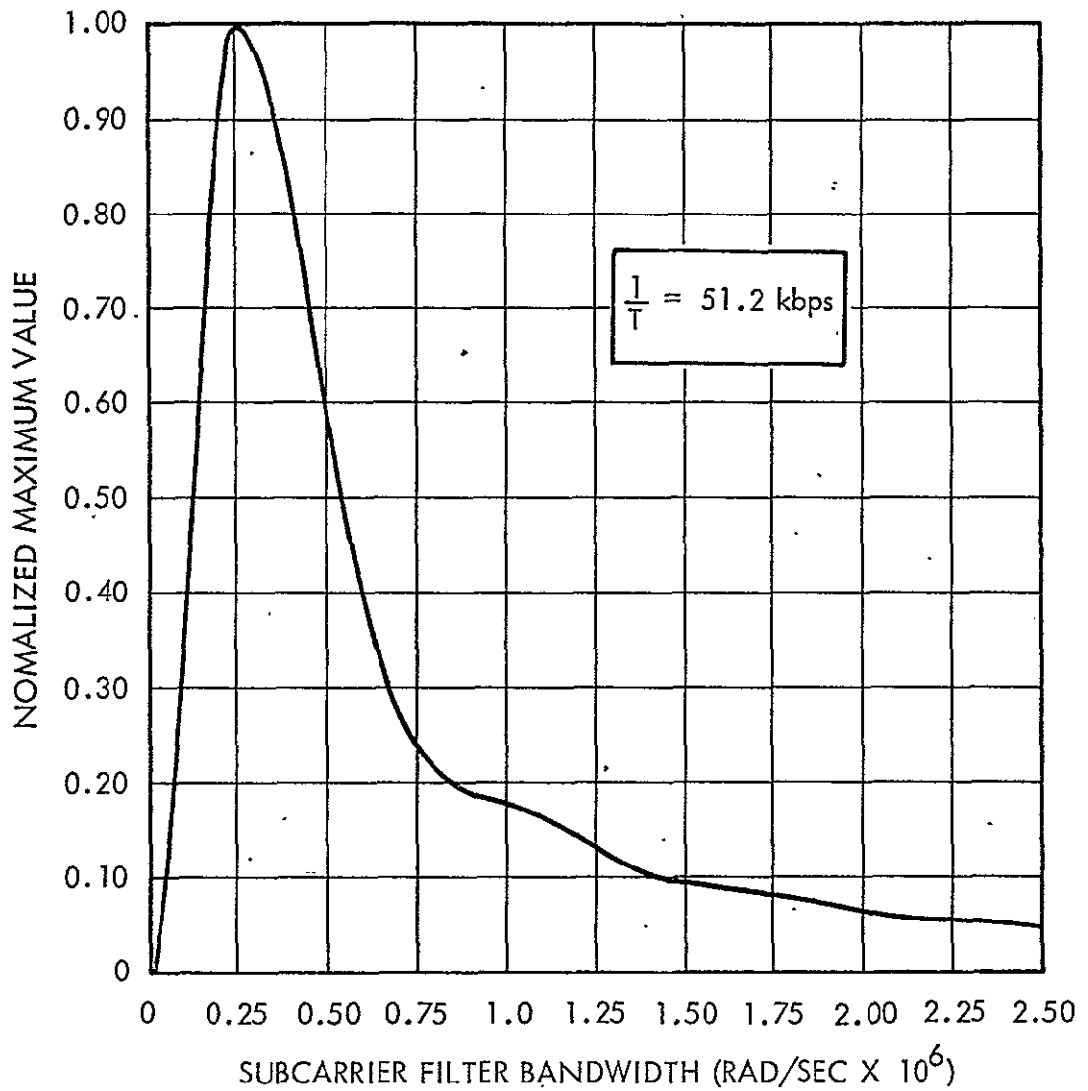


Figure 5-3. Normalized Maximum Value of the Envelope Function versus TM Subcarrier Filter Bandwidth

6. A PROPOSED SPUR REDUCTION TECHNIQUE

A proposed method for reducing the S/C ratio is presented in this section. The technique is based upon an expression for the TM PM/PM downlink signal derived in Appendix B (Equation (B-5)) .

$$e(t) = A \sin(\omega_c t) - A a \beta^2 \sin(\omega_c t) g^2(t) + A \cos(\omega_c t) \sin(\beta g(t)) \quad (6-1)$$

where $A^2/2$ is the unmodulated carrier power, β is the TM modulation index, ω_c is the carrier radian frequency, $g(t)$ is the filtered biphas modulated subcarrier, and a is a constant ($a = 0.4368$) derived in Appendix D.

It is shown in Appendix B that only the first two terms in Equation (6-1) contribute to the expression for the S/C ratio, and that only the last term contains the desired TM information. In particular, the second term is the source of the TM spurs. (A more exact statement would be that the source of the spurs is the sum of all the even powers of $g(t)$. However, it is shown in Appendix D that for values of β less than 1.5 the squared term is dominant and that truncation after the squared term causes little error.) It should be possible then to effect a significant reduction in the S/C ratio by removing the second term in Equation (6-1) from the downlink signal. Figure 6-1 is a block diagram showing the proposed spur reduction technique. The output of the band-pass filter is $g(t)$. This signal is normally sent to the PM mixer where it phase modulates the S-band carrier (Section 2). However, in Figure 2-8, it is split and sent into a lower loop containing a squaring device, a balanced mixer, and an amplifier.* The output of the square law detector is $(k_s/2)g^2(t)$, where k_s is the gain of the detector. The balanced mixer (gain = k_m) forms the product $(Ak_s k_m/2\sqrt{2})\sin(\omega_c t)g^2(t)$. This term is then given

* The amplifier may also be placed at the output of the square law detector.

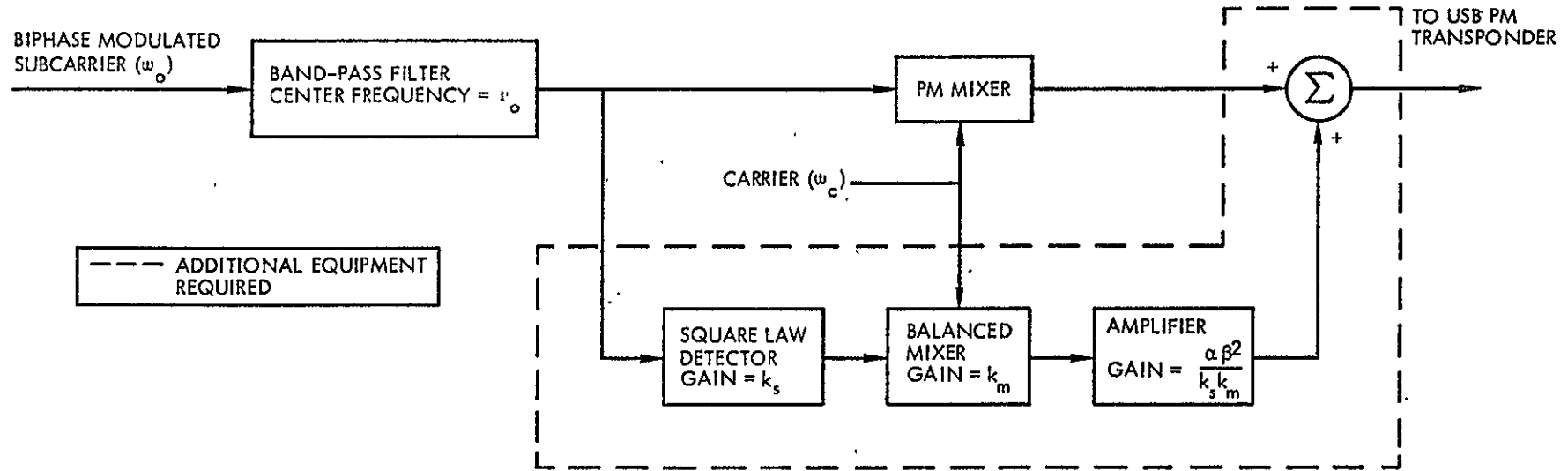


Figure 6-1. Proposed Spur Reduction Technique

the proper coefficient ($A a\beta^2/2\sqrt{2}$) by the amplifier. The output of the lower loop is then

$$\text{output} = \left(\frac{A a\beta^2}{2\sqrt{2}} \right) \sin(\omega_c t) g^2(t) \quad (6-2)$$

When this signal is added* to the output of the PM mixer the signal sent to the USB transponder becomes

$$e'(t) = \frac{A}{\sqrt{2}} \sin(\omega_c t) + \frac{A}{\sqrt{2}} \cos(\omega_c t) \sin\left[\frac{\beta}{\sqrt{2}} g(t)\right] \quad (6-3)$$

Examination of $e'(t)$ shows that the spur generating terms have been removed.

The amplifier shown in Figure 6-1 must have a gain of exactly $a\beta^2/k_s k_m$ for complete spur elimination. Significant reduction in the spurs may also be obtained with amplifier gains close to that value. Figure 6-2 shows the spur reduction as a function of "gain ratio", where

$$\text{gain ratio} = \frac{\text{actual gain}}{\text{gain required for complete spur elimination}}$$

The reduction in the S/C ratio is also a function of the TM modulation index β , as is shown in Figure 6-2. For example, with a modulation index of 1.3 and a gain ratio of 0.9, an approximate 25 dB reduction in the S/C ratio could be obtained. Thus, if one of the spurs was originally at -29 dB relative to the S-band carrier it would now be down -54 dB relative to the carrier.

It is shown in Appendix B that the second term in Equation (6-1) also reduces the S-band carrier power. Thus, if the term is removed from the downlink signal for the purpose of spur reduction an increase in the carrier power could also be expected. However, power splitting in the lower loop has the opposite effect. The net result is shown in Figure 6-3. It is a plot of carrier power increase resulting from the use of the spur

* It is assumed that the signal delay in the additional equipment is exactly that experienced in the PM mixer.

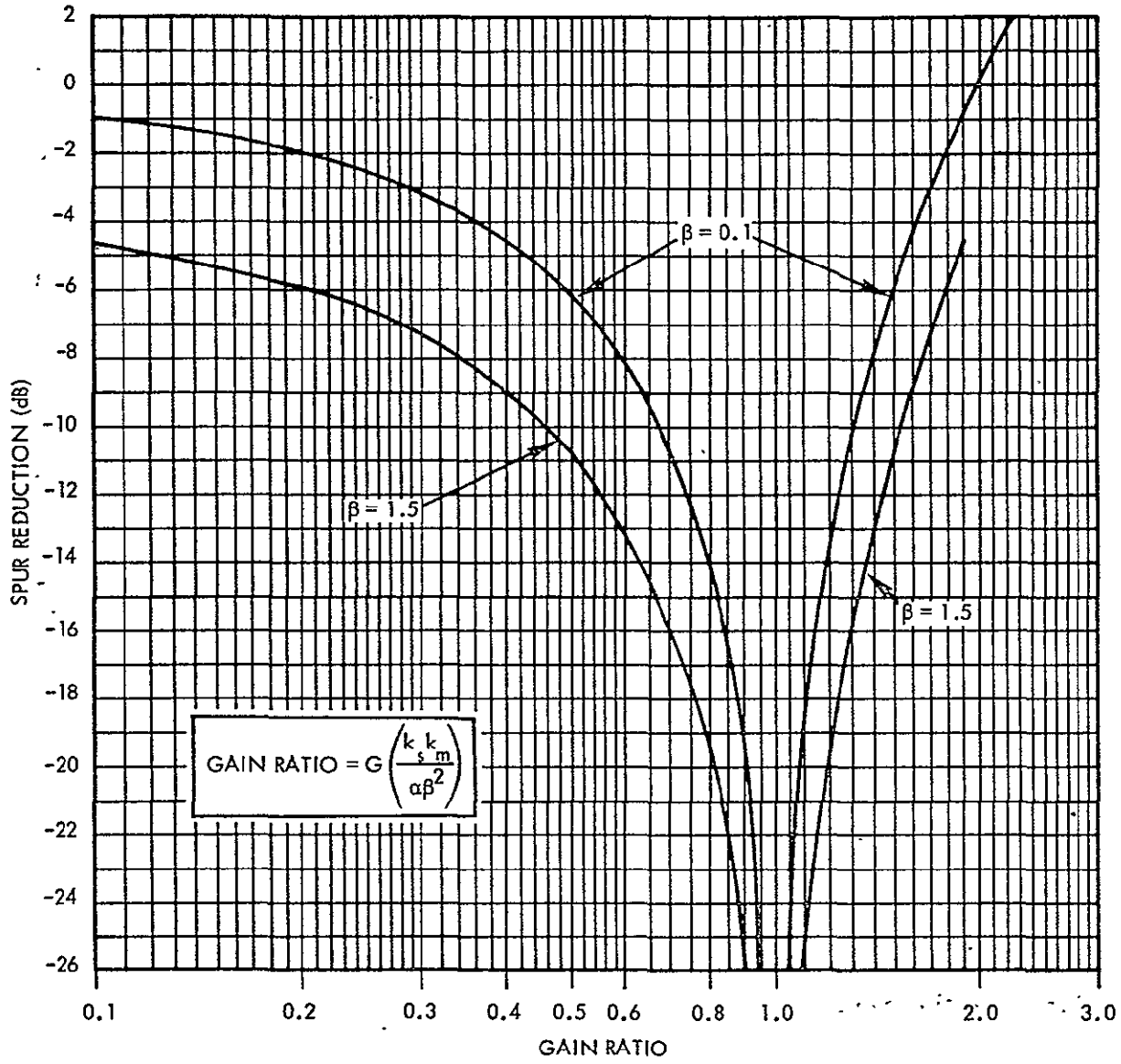


Figure 6-2. Spur Reduction versus Gain Ratio

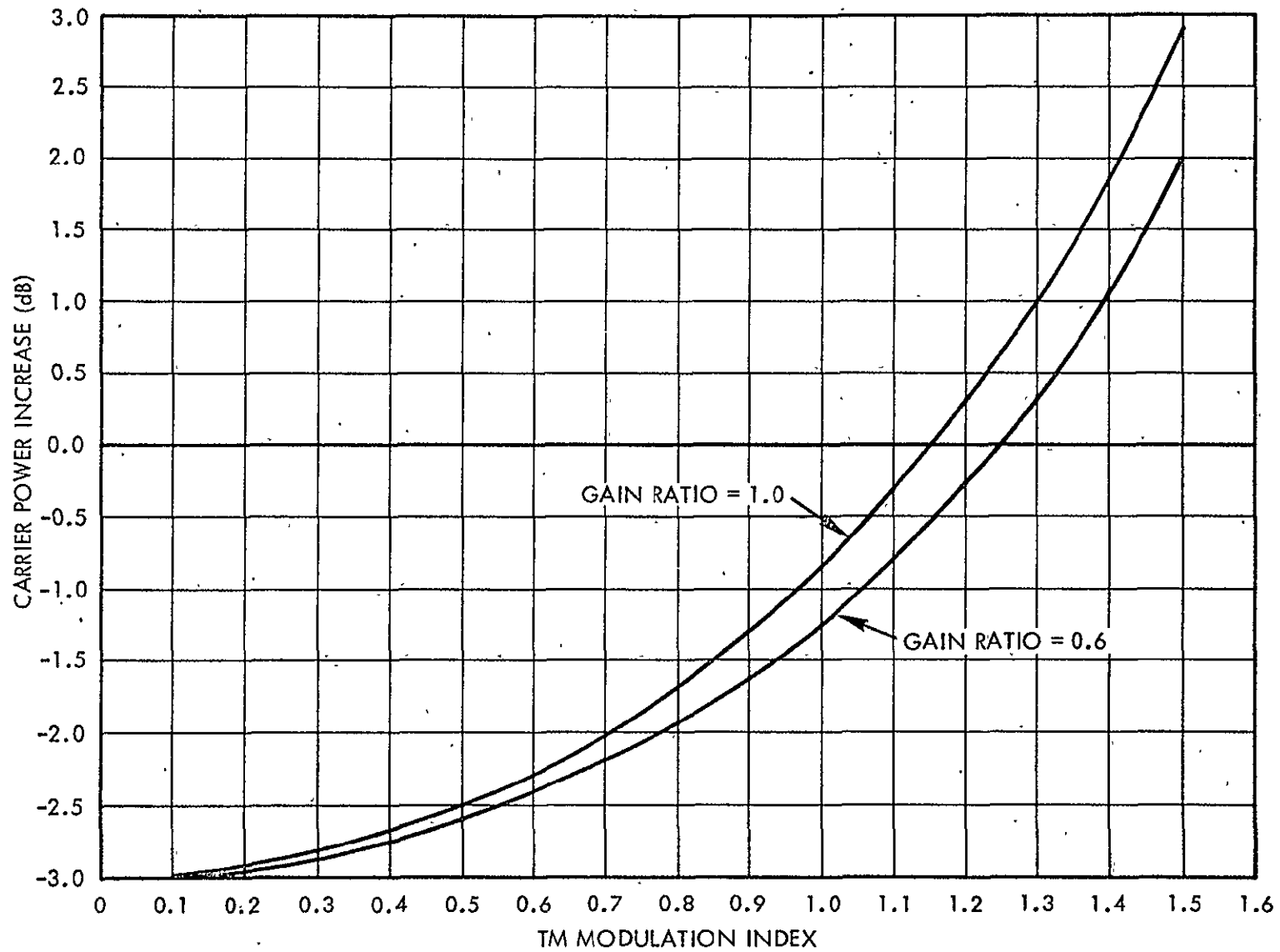


Figure 6-3. Carrier Power Increase versus the TM Modulation Index for Two Values of the Amplifier Gain Ratio

reduction system versus the TM modulation index. The amount of carrier increase is also a function of the gain ratio, as is shown in Figure 6-3. If β is 1.3 and the gain ratio is close to 1.0, Figure 6-3 shows that an approximate 1.0 dB increase in carrier power could be expected.

The proposed spur reduction system will cause carrier and sub-carrier power losses due to power splitting in the lower loop, as shown in Figure 6-1. However, these losses can be eliminated by selective amplification of the proper signals so that the resulting total transmitted power from the transponder is the same as it was before the addition of the spur reduction system. Under this condition, the carrier power will be increased by approximately 4 dB ($\beta = 1.3$), with no decrease in the TM sideband power. The increase in carrier power is caused by the transfer of power from the spurs to the S-band carrier.

7. COMPUTER SIMULATION OF THE TM PM/PM MODULATION PROCESS

A computer program has been written in FORTRAN V for use with the Exec II operating system on the SRU 1108 digital computer. The program simulates the phase modulation of a carrier by a band-limited biphasic modulated subcarrier and calculates the amplitude spectrum of the resulting signal.

The program was used primarily as an independent check on the mathematical analysis presented in this report, but it may also be used to predict the TM spur amplitudes for values of the subcarrier modulation index greater than 1.5. (The equations in Sections 3 and 4 are valid only for values of β less than 1.5.)

Figure 7-1 is a diagram of the equations used in the program. All of the parameters (Ω , β , T, etc.) may be changed as desired. The PCM-NRZ code is generated by the computer as a random sequence of ones and zeros.

Figure 7-2 is a computer generated spectrum of the TM PM/PM signal $\left(\frac{1}{NT} |H(\omega)|^2\right)$ in Figure 7-1). Note that the spurs around the carrier are located at integral multiples of the TM bit rate.

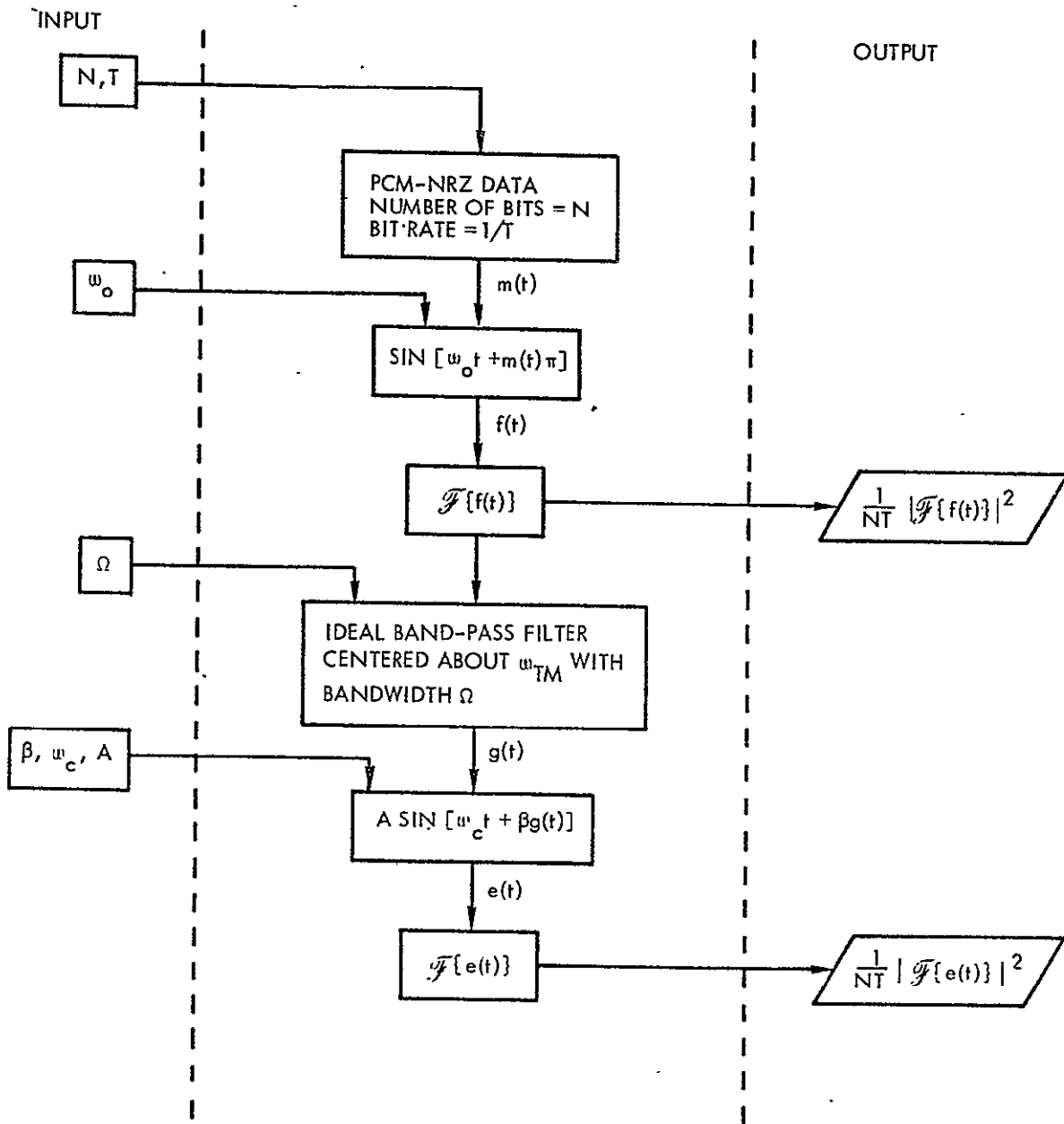


Figure 7-1. Diagram of the Equations Used in the Computer Simulation of the TM PM/PM Process

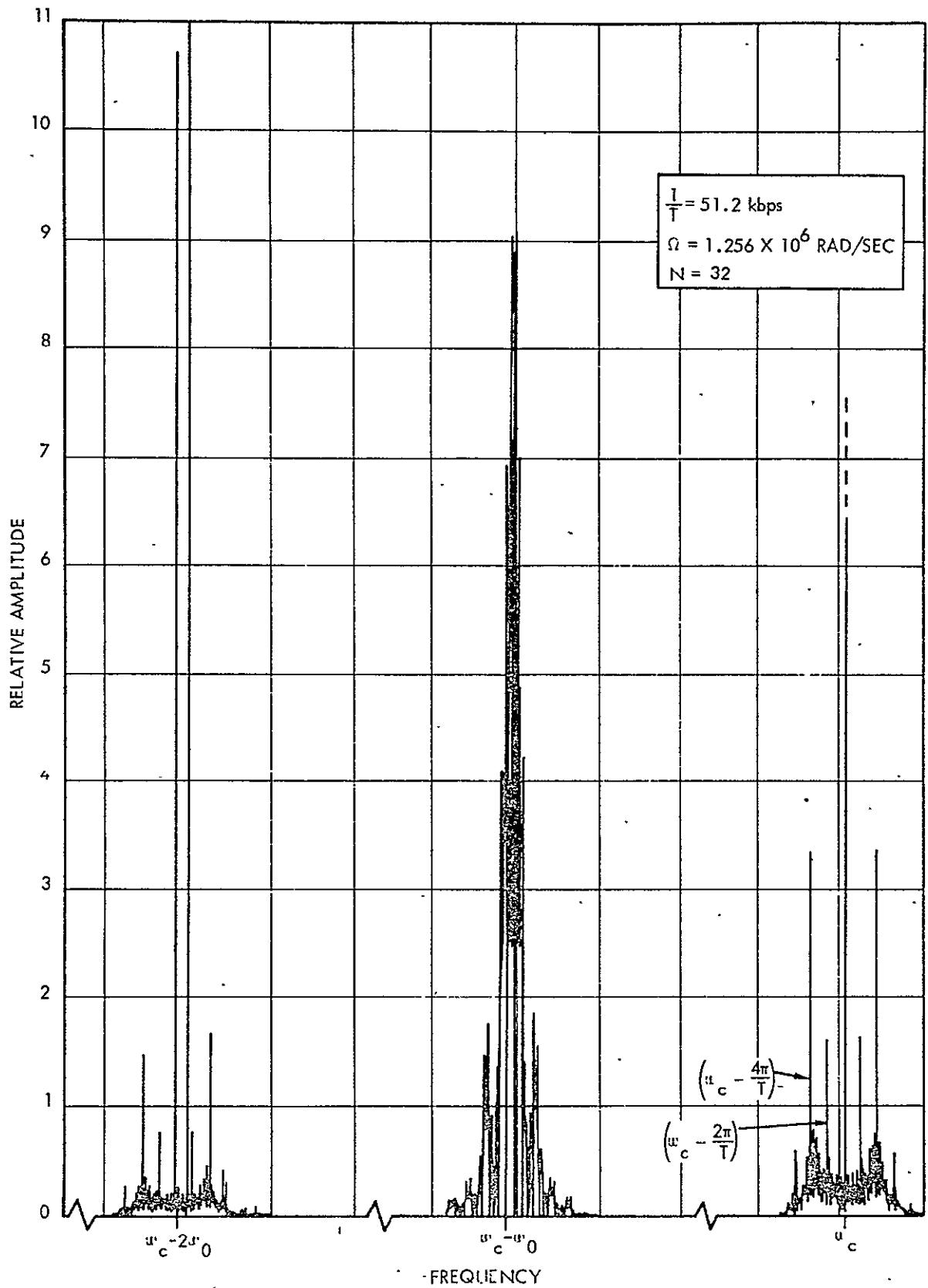


Figure 7-2. Computer Generated Spectrum of the TM PM/PM Signal

8. SUMMARY OF RESULTS

The basic TM PM/PM modulation process used on CSM downlink S-band PM modes 1, 2, 3, 4, 5, 8, and 9 and LM downlink PM modes 1, 2, 3, 4, 7, and 8 has been studied in this report. The results of the study indicate that TM spurs will be present in the signal spectrum of each CSM and LM mode listed above and will also be present whenever the S-band carrier is phase modulated with a filtered, biphasic modulated subcarrier. It is the combined effects of the two operations, band limitation of the telemetry and phase modulation of the S-band carrier, which generate the TM spurs.

The spurs have been shown to be located at integral multiples of the TM bit rate about the S-band carrier and their amplitude relative to the S-band carrier to be a function of (1) the TM subcarrier modulation index, (2) the subcarrier filter bandwidth, and (3) the TM bit rate. The expression relating the above three parameters to the S/C ratio has been derived, and a table of S/C ratios have been provided in Appendix F.

A technique capable of producing significant reductions in the S/C ratio (in addition to an increase in the S-band carrier power) has been proposed. Reductions of approximately 25dB in the S/C ratio have been shown to be possible with existing Apollo CSM and LM parameters.

Figure 8-1 is a plot showing the S/C ratio predicted by equations derived in this report, and the S/C ratio obtained by computer simulation of the TM PM/PM modulation process. Both are plotted for a BPB product of 24.6. If Figure 7-1 is compared with Figure D-1 it can be seen that deviations in the S/C ratio are consistent with the approximation of $\cos[\beta g(t)]$ used in the derivation of the predicted S/C ratio.

Amplitude modulation (AM) in the output of the subcarrier bandpass filter has also been discussed, and an expression relating the TM bit rate and the subcarrier filter bandwidth to the resulting AM envelope has been derived in Appendix C.

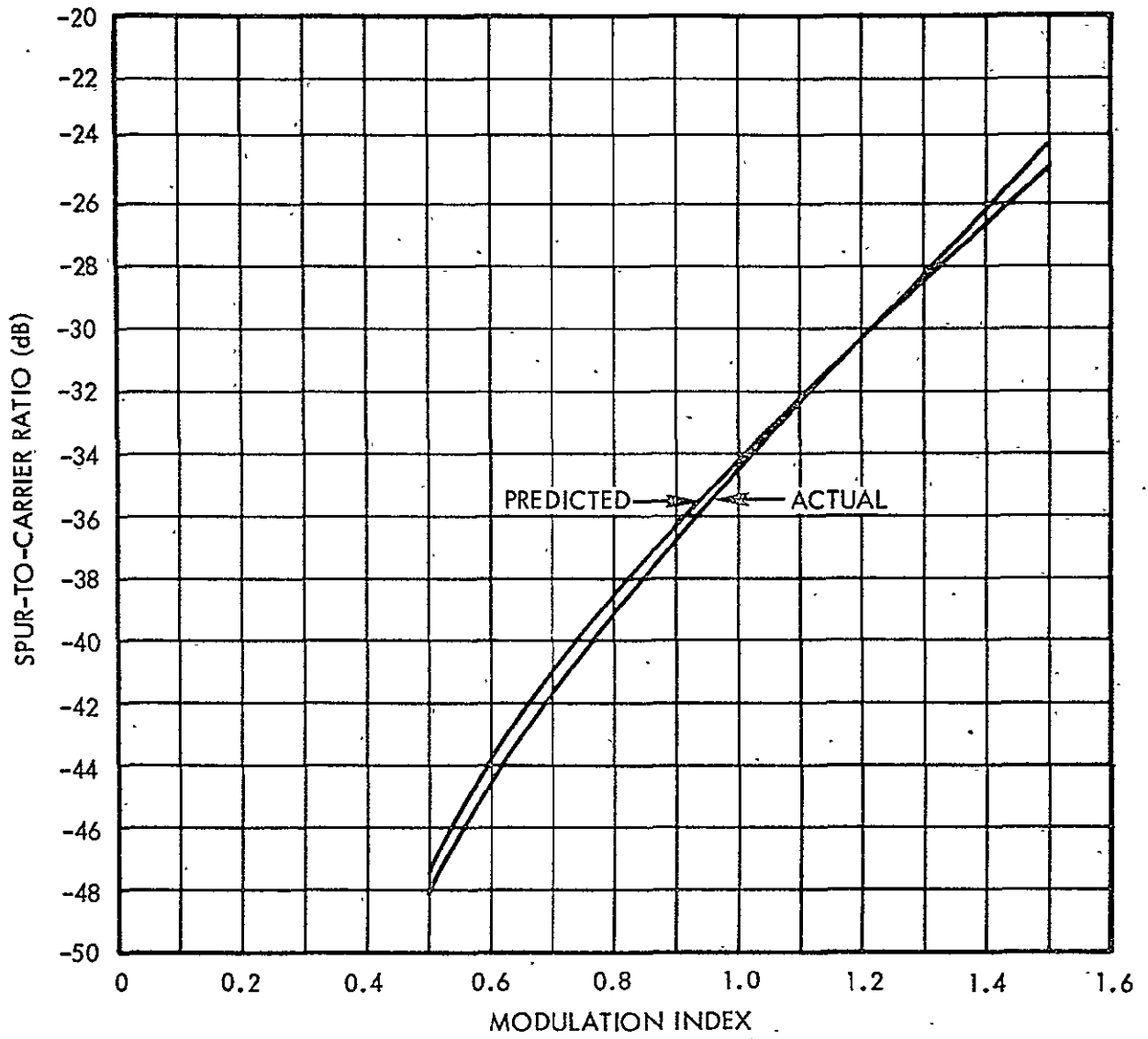


Figure 8-1. Predicted and Actual S/C Ratios versus TM Modulation Index for $T\Omega = 24.6$

APPENDIX A

THE FOURIER TRANSFORM OF A SINUSOID PHASE MODULATED BY A
TIME LIMITED, APERIODIC PCM-NRZ CODE

The Fourier transform of the function $f(t)$ is defined by the integral

$$F(\omega) = \int_{-\infty}^{\infty} f(t)e^{-j\omega t} dt \quad (A-1)$$

If $F(\omega)$ and $f(t)$ are transform pairs, then the Fourier transform of $f(t - t_0)$ is given by

$$\mathcal{F}\{f(t - t_0)\} = F(\omega)e^{-j\omega t_0} \quad (A-2)$$

If $G(\omega)$ and $g(t)$ are transform pairs, then the Fourier transform of the product $f(t)g(t)$ is given by

$$\mathcal{F}\{f(t)g(t)\} = \frac{1}{2\pi} \int_{-\infty}^{\infty} F(\alpha)G(\omega - \alpha) d\alpha \quad (A-3)$$

Let the biphase modulated sinusoid be given by

$$f(t) = \sin \left[\omega_0 t + m(t)\pi \right] \quad (A-4)$$

where $m(t)$ (Figure A-1) is the random PCM-NRZ code having the value 0 or 1 with equal probability, and $\omega_0 = k\left(\frac{2\pi}{T}\right)$ $k = 1, 2, 3, \dots$

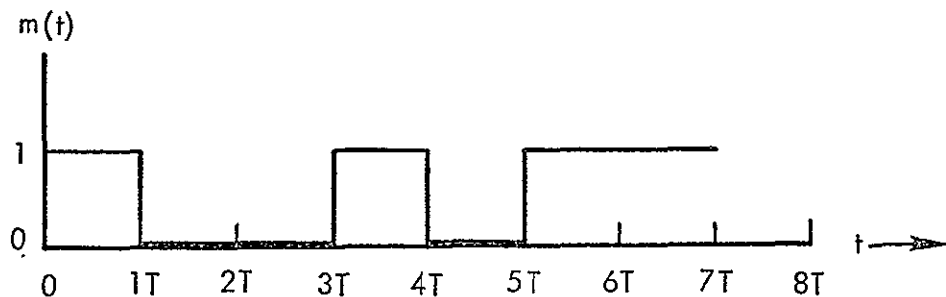


Figure A-1. $m(t)$ versus Time

The function may also be written

$$f(t) = m'(t) \sin(\omega_0 t) \quad (A-5)$$

where

$$m'(t) = \begin{cases} 1, & \text{if } m(t) = 0 \\ -1, & \text{if } m(t) = 1 \end{cases} \quad (A-6)$$

Let $g(t, \alpha_n)$ be defined as

$$g(t, \alpha_n) = \sum_{n=0}^{N-1} \alpha_n P_T \left[t - (n + \frac{1}{2})T \right] \quad (A-7)$$

where N is the number of bits in the PCM-NRZ code and $P_T(t)$ is a unit pulse centered at the origin having width T . The constant α_n is defined as

$$\alpha_n = \begin{cases} 1, & \text{if the } n\text{th bit is 1} \\ -1, & \text{if the } n\text{th bit is 0} \end{cases} \quad (A-8)$$

Thus,

$$g(t, \alpha_n) = m'(t) \quad (A-9)$$

And, from Equation (A-5),

$$f(t) = g(t, \alpha_n) \sin(\omega_0 t) \quad (A-10)$$

To indicate the functional relationship between $f(t)$ and α_n , let

$$f(t) = f(t, \alpha_n) \quad (A-11)$$

Then,

$$f(t, \alpha_n) = \left\{ \sum_{n=0}^{N-1} \alpha_n P_T \left[t - (n + \frac{1}{2})T \right] \right\} \sin(\omega_0 t) \quad (A-12)$$

$$f(t, \alpha_n) = \sum_{n=0}^{N-1} \alpha_n \sin(\omega_0 t) P_T \left[t - (n + \frac{1}{2})T \right] \quad (A-13)$$

$$= \sum_{n=0}^{N-1} \alpha_n h(n, t) \quad (A-14)$$

where

$$h(n, t) = \sin(\omega_0 t) P_T \left[t - (n + \frac{1}{2})T \right] \quad (A-15)$$

Referring to Equation (A-2), the Fourier transform of $P_T \left[t - (n + \frac{1}{2})T \right]$ is given by

$$\mathcal{F} \left\{ P_T \left[t - (n + \frac{1}{2})T \right] \right\} = \mathcal{F} \left\{ P_T(t) \right\} e^{-j\omega(n + \frac{1}{2})T} \quad (A-16)$$

It may be shown that

$$\mathcal{F} \left\{ P_T(t) \right\} = \frac{2 \sin \left(\frac{\omega T}{2} \right)}{\omega} \quad (A-17)$$

Thus

$$\mathcal{F} \left\{ P_T \left[t - (n + \frac{1}{2})T \right] \right\} = \frac{2 \sin \left(\frac{\omega T}{2} \right)}{\omega} e^{-j\omega(n + \frac{1}{2})T} \quad (A-18)$$

Referring to Equations (A-3) and (A-18), the Fourier transform of $h(n, t)$ is

$$\mathcal{F} \left\{ h(n, t) \right\} = \frac{1}{2\pi} \int_{-\infty}^{\infty} j\pi \left[\delta(\alpha + \omega_0) - \delta(\alpha - \omega_0) \right] \frac{2 \sin \frac{(\omega - \alpha)T}{2}}{\omega - \alpha} e^{-j(\omega - \alpha)(n + \frac{1}{2})T} d\alpha \quad (A-19)$$

$$= j \left[\frac{\sin \frac{(\omega + \omega_0)T}{2}}{\omega + \omega_0} e^{-j(\omega + \omega_0)(n + \frac{1}{2})T} - \frac{\sin \frac{(\omega - \omega_0)T}{2}}{\omega - \omega_0} e^{-j(\omega - \omega_0)(n + \frac{1}{2})T} \right] \quad (A-20)$$

$$\mathcal{F}\{h(n,t)\} = (j)^{2k+1} \left[\frac{\sin\left(\frac{\omega T}{2}\right)}{\omega + \omega_0} - \frac{\sin\left(\frac{\omega T}{2}\right)}{\omega - \omega_0} \right] e^{-j(n + \frac{1}{2})T\omega} \quad (\text{A-21})$$

$$= 2(j)^{2k-1} \sin\left(\frac{\omega T}{2}\right) \left[\frac{\omega_0}{\omega^2 - \omega_0^2} \right] e^{-j(n + \frac{1}{2})T\omega} \quad (\text{A-22})$$

From Equations (A-14) and (A-22), the Fourier transform of the biphasemodulated sinusoid is

$$F(\omega, \alpha_n) = \mathcal{F}\{f(t, \alpha_n)\} \quad (\text{A-23})$$

$$= \sum_{n=0}^{N-1} \alpha_n 2(j)^{2k-1} \sin\left(\frac{\omega T}{2}\right) \left[\frac{\omega_0}{\omega^2 - \omega_0^2} \right] e^{-j(n + \frac{1}{2})T\omega} \quad (\text{A-24})$$

$$= 2(j)^{2k-1} \sin\left(\frac{\omega T}{2}\right) \left[\frac{\omega_0}{\omega^2 - \omega_0^2} \right] \sum_{n=0}^{N-1} \alpha_n e^{-j(n + \frac{1}{2})T\omega} \quad (\text{A-25})$$

$$= 2(-1)^{k+1} \sin\left(\frac{\omega T}{2}\right) \left[\frac{\omega_0}{\omega^2 - \omega_0^2} \right] \cdot$$

$$\cdot \left[\sum_{n=0}^{N-1} \alpha_n \sin(n + \frac{1}{2})T\omega + j \sum_{n=0}^{N-1} \alpha_n \cos(n + \frac{1}{2})T\omega \right] \quad (\text{A-26})$$

Note that $F(\omega, \alpha_n)$ is a function of the random variables $\alpha_0, \alpha_1, \dots, \alpha_{N-1}$

From Equation (A-26), the real part of $F(\omega, \alpha_n)$ is

$$R(\omega, \alpha_n) = 2(-1)^{k+1} \sin\left(\frac{\omega T}{2}\right) \left[\frac{\omega_0}{\omega^2 - \omega_0^2} \right] \sum_{n=0}^{N-1} \alpha_n \sin(n + \frac{1}{2})T\omega \quad (\text{A-27})$$

And the imaginary part is

$$X(\omega, \alpha_n) = 2(-1)^{k+1} \sin\left(\frac{\omega T}{2}\right) \left[\frac{\omega_0}{\omega^2 - \omega_0^2} \right] \sum_{n=0}^{N-1} \alpha_n \cos\left(n + \frac{1}{2}\right) T \omega \quad (\text{A-28})$$

$R(\omega, \alpha_n)$ and $X(\omega, \alpha_n)$ are shown in Figures A-2 and A-3 for positive values of ω .

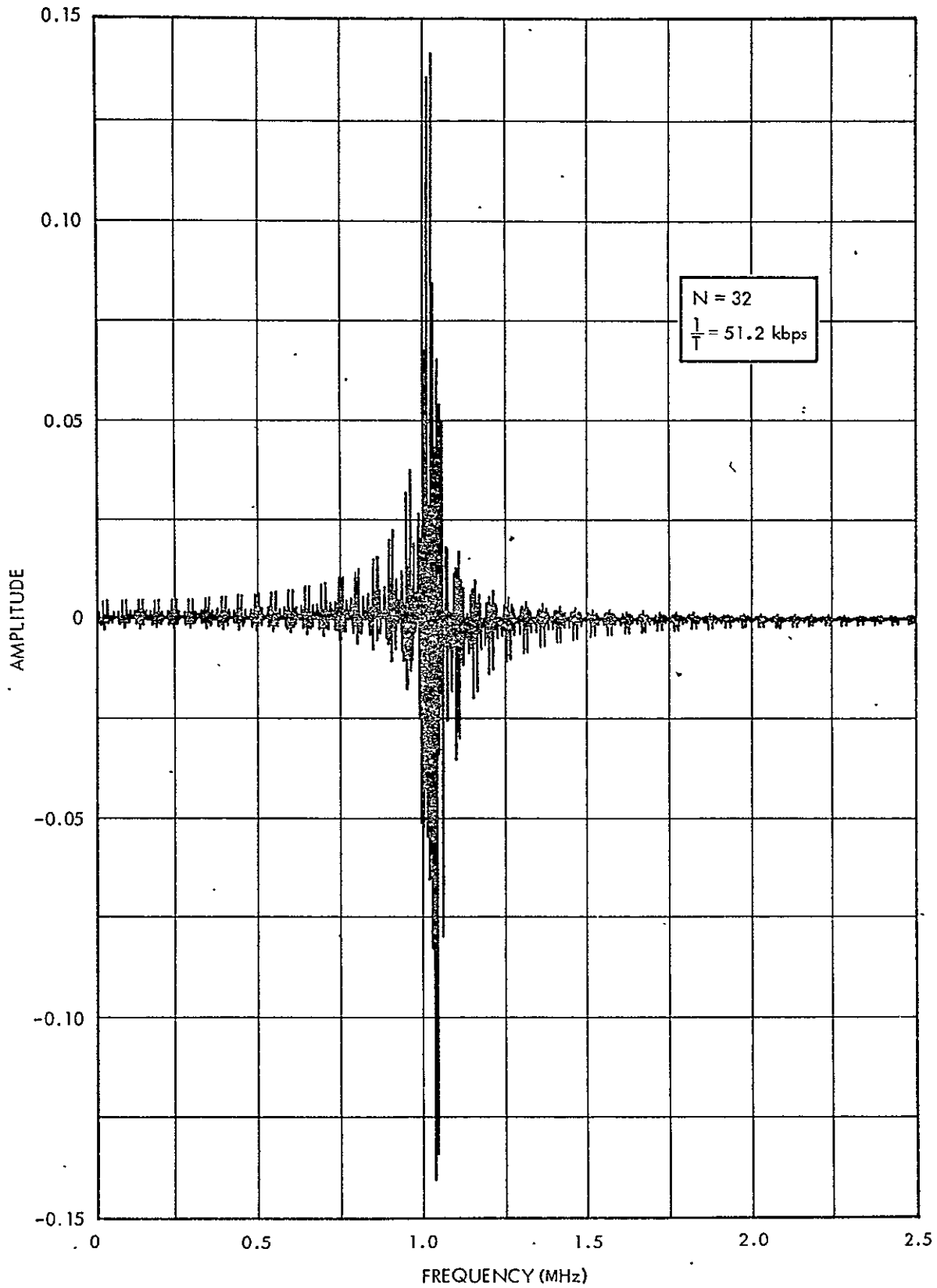


Figure A-2. Real Part of $F(\omega, \alpha_n)$ versus Frequency ($f_0 = 1.024 \text{ MHz}$)

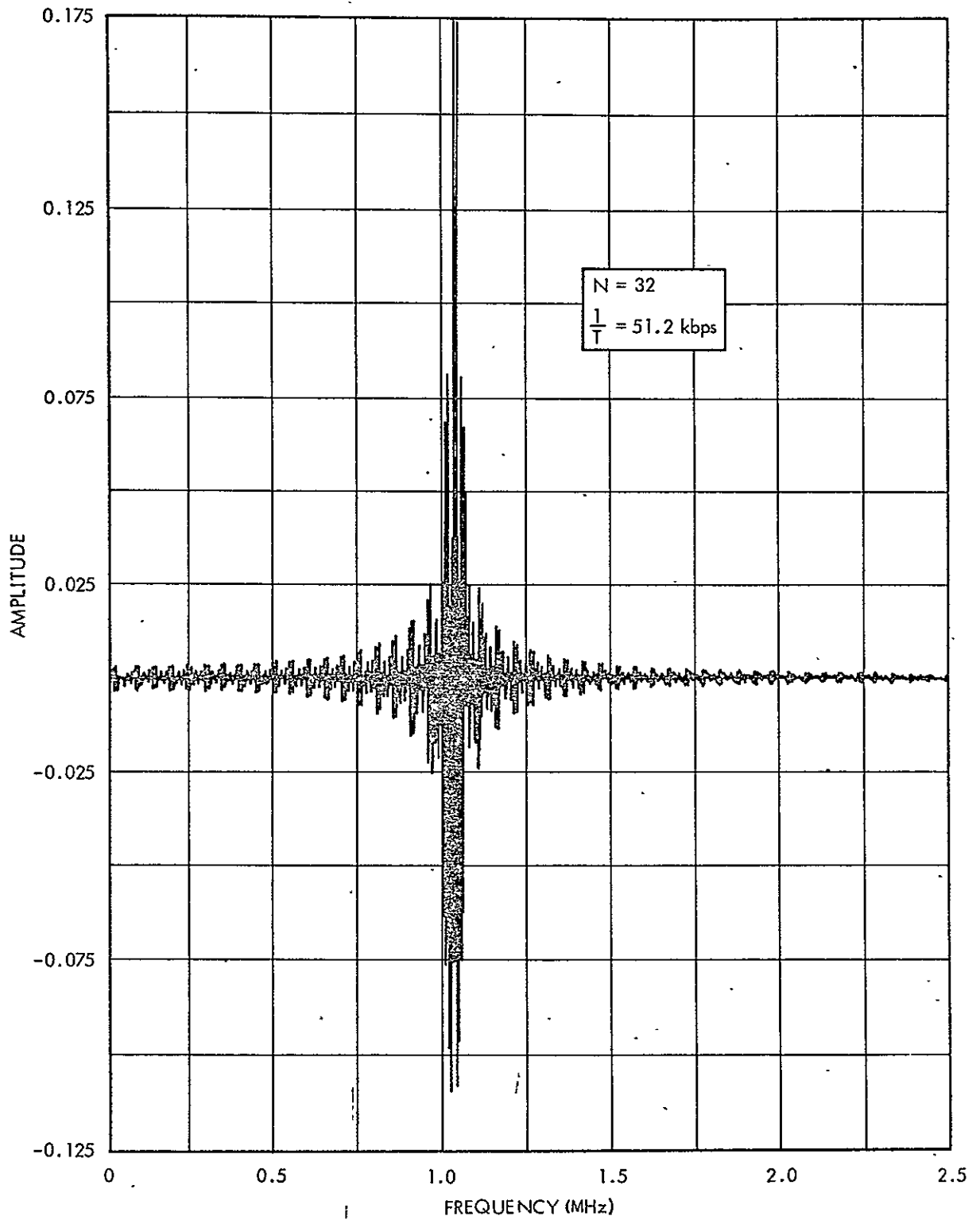


Figure A-3. Imaginary Part of $F(\omega, \alpha_n)$ versus Frequency ($f_0 = 1.024 \text{ MHz}$)

APPENDIX B

THE RELATIVE SPUR AMPLITUDES AS A FUNCTION OF SUBCARRIER FILTER BANDWIDTH, TM MODULATION INDEX, AND TM BIT RATE

The phase modulated signal to be analyzed is

$$e(t, \alpha_n) = A \sin [\omega_c t + \beta g(t, \alpha_n)], \quad 0 \leq t \leq NT, \quad (\text{B-1})$$

where ω_c is the carrier radian frequency and β is the subcarrier modulation index. The α_n in the argument of $e(t, \alpha_n)$ and $g(t, \alpha_n)$ is described in detail in Appendix A. The modulating function $g(t, \alpha_n)$ is obtained from the biphasic modulated subcarrier $f(t, \alpha_n)$, Equation (A-4), by band-limiting $f(t, \alpha_n)$ with an ideal band-pass filter of bandwidth Ω centered at the subcarrier radian frequency ω_c .

The assumptions used in the analysis of $e(t, \alpha_n)$ are the following.

- a) The carrier radian frequency ω_c is greater than one-half the TM subcarrier radian frequency ω_o .
- b) The TM modulation index β is less than 1.5.

An expansion of Equation (B-1) gives

$$e(t, \alpha_n) = A \sin (\omega_c t) \cos [\beta g(t, \alpha_n)] + A \cos (\omega_c t) \sin [\beta g(t, \alpha_n)] \quad (\text{B-2})$$

If β is less than 1.5, then

$$e(t, \alpha_n) \approx A \sin (\omega_c t) [1 - a \beta^2 g^2(t, \alpha_n)] + A \cos (\omega_c t) [\beta g(t, \alpha_n)] \quad (\text{B-3})$$

where, as is shown in Appendix D,

$$a = 0.4368 \quad (\text{B-4})$$

A further expansion of Equation (B-3) gives

$$e(t, \alpha_n) = A \sin (\omega_c t) - A a \beta^2 \sin (\omega_c t) g^2(t, \alpha_n) + A \beta \cos (\omega_c t) g(t, \alpha_n) \quad (\text{B-5})$$

where the approximation indicated in Equation (B-3) will be considered an equality.

Only the second term in Equation (B-5) contributes to the spectrum of $e(t, \alpha_n)$ in the neighborhood of $\omega_c \pm k \left(\frac{2\pi}{T}\right)$, $k = 1, 2, \dots$. The Fourier transform of $g^2(t, \alpha_n)$ is

$$G_2(\omega, \alpha_n) = \mathcal{F}\{g^2(t, \alpha_n)\} \quad (B-6)$$

$$= \frac{1}{2\pi} G(\omega, \alpha_n) * G(\omega, \alpha_n) \quad (B-7)$$

where * indicates convolution, and

$$G(\omega, \alpha_n) = \mathcal{F}\{g(t, \alpha_n)\} \quad (B-8)$$

Recall that $g(t, \alpha_n)$ is the band-limited version of $f(t, \alpha_n)$ described in Appendix A. Thus,

$$G(\omega, \alpha_n) = P_\Omega(\omega) \mathcal{F}\{f(t, \alpha_n)\} \quad (B-9)$$

$$= 2(-1)^{k+1} P_\Omega(\omega) \sin\left(\frac{TW}{2}\right) \left[\frac{\omega_0}{\omega^2 - \omega_0^2} \right]$$

$$\cdot \left[\sum_{n=1}^{N-1} \alpha_n \sin\left[(n + 1/2) T \omega\right] + j \sum_{n=0}^{N-1} \alpha_n \cos\left[(n + 1/2) T \omega\right] \right] \quad (B-10)$$

where ω_0 is the subcarrier radian frequency, and

$$P_\Omega(\omega) = \mu_\Omega(\omega - \omega_0) + \mu_\Omega(\omega + \omega_0) \quad (B-11)$$

and $\mu_\Omega(\omega)$ is a unit pulse centered at the origin having width Ω .

Equation (B-10) may be written as

$$G(\omega, \alpha_n) = R_G(\omega, \alpha_n) + j X_G(\omega, \alpha_n) \quad (B-12)$$

where

$$R_G(\omega, \alpha_n) = 2(-1)^{k+1} P_\Omega(\omega) \sin\left(\frac{T\omega}{2}\right) \left[\frac{\omega_0}{\omega^2 - \omega_0^2} \right] \cdot \sum_{n=0}^{N-1} \alpha_n \sin\left[\left(n + \frac{1}{2}\right) T\omega\right] \quad (B-13)$$

$$X_G(\omega, \alpha_n) = 2(-1)^{k+1} P_\Omega(\omega) \sin\left(\frac{T\omega}{2}\right) \left[\frac{\omega_0}{\omega^2 - \omega_0^2} \right] \cdot \sum_{n=0}^{N-1} \alpha_n \cos\left[\left(n + \frac{1}{2}\right) T\omega\right] \quad (B-14)$$

Substitution of Equation (B-12) into Equation (B-7) gives

$$G_2(\omega, \alpha_n) = \frac{1}{2\pi} \left[R_G(\omega, \alpha_n) + j X_G(\omega, \alpha_n) \right] * \left[R_G(\omega, \alpha_n) + j X_G(\omega, \alpha_n) \right] \quad (B-15)$$

$$= \frac{1}{2\pi} \left[R_G(\omega, \alpha_n) * R_G(\omega, \alpha_n) - X_G(\omega, \alpha_n) * X_G(\omega, \alpha_n) \right] + \frac{j}{\pi} R_G(\omega, \alpha_n) * X_G(\omega, \alpha_n) \quad (B-16)$$

It may be shown that

$$\frac{1}{2} \left[R_G(\omega, \alpha_n) * R_G(\omega, \alpha_n) - X_G(\omega, \alpha_n) * X_G(\omega, \alpha_n) \right] \gg R_G(\omega, \alpha_n) * X_G(\omega, \alpha_n) \quad (B-17)$$

Thus,

$$G_2(\omega, \alpha_n) \approx \frac{1}{2\pi} \left[R_G(\omega, \alpha_n) * R_G(\omega, \alpha_n) - X_G(\omega, \alpha_n) * X_G(\omega, \alpha_n) \right] \quad (B-18)$$

It may also be shown that near $\omega = \omega_c + k \left(\frac{2\pi}{T}\right)$, $k = 1, 2, \dots$

$$\begin{aligned}
 R_G(\omega, \alpha_n) * R_G(\omega, \alpha_n) &\cong -2 P_\Omega(\omega) \left[\frac{\sin\left(\frac{T\omega}{2}\right)}{\omega + \omega_0} \right] \\
 \cdot \sum_{n=0}^{N-1} \alpha_n \sin\left[\left(n + \frac{1}{2}\right) T\omega\right] * P_\Omega(\omega) &\left[\frac{\sin\left(\frac{T\omega}{2}\right)}{\omega - \omega_0} \right] \\
 \cdot \sum_{n=0}^{N-1} \alpha_n \sin\left[\left(n + \frac{1}{2}\right) T\omega\right] & \qquad \qquad \qquad (B-19)
 \end{aligned}$$

and that

$$\begin{aligned}
 X_G(\omega, \alpha_n) * X_G(\omega, \alpha_n) &\cong -2 P_\Omega(\omega) \left[\frac{\sin\left(\frac{T\omega}{2}\right)}{\omega + \omega_0} \right] \\
 \cdot \sum_{n=0}^{N-1} \alpha_n \cos\left[\left(n + \frac{1}{2}\right) T\omega\right] * P_\Omega(\omega) &\left[\frac{\sin\left(\frac{T\omega}{2}\right)}{\omega - \omega_0} \right] \\
 \cdot \sum_{n=0}^{N-1} \alpha_n \cos\left[\left(n + \frac{1}{2}\right) T\omega\right] & \qquad \qquad \qquad (B-20)
 \end{aligned}$$

Equations (B-19) and (B-20) are long and rather complicated when written in integral form. For that reason, only Equation (B-19) will be examined in detail. The results for Equation (B-20) will be presented without a derivation.

An expansion of Equation (B-19) gives

$$R_G(\omega, \alpha_n) * R_G(\omega, \alpha_n) = \frac{-1/2}{\omega + \omega_0} P_\Omega(\omega) \left[\sum_{n=0}^{N-1} \alpha_n \cos(nT\omega) \right. \\ \left. - \sum_{n=0}^{N-1} \alpha_n \cos[(n+1)T\omega] \right] * \frac{1}{\omega - \omega_0} \cdot \\ \cdot \left[\sum_{n=0}^{N-1} \alpha_n \cos(nT\omega) - \sum_{n=0}^{N-1} \alpha_n \cos[(n+1)T\omega] \right] \quad (B-21)$$

$$= I_1(\omega, \alpha_n) + I_2(\omega, \alpha_n) + I_3(\omega, \alpha_n) \\ + I_4(\omega, \alpha_n) \quad (B-22)$$

where

$$I_1(\omega, \alpha_n) = -P_\Omega(\omega) \frac{1/2}{\omega + \omega_0} \sum_{n=0}^{N-1} \alpha_n \cos(nT\omega) * \frac{1}{\omega - \omega_0} \sum_{n=0}^{N-1} \alpha_n \cos(nT\omega) \quad (B-23)$$

$$I_2(\omega, \alpha_n) = -P_\Omega(\omega) \frac{1/2}{\omega + \omega_0} \sum_{n=0}^{N-1} \alpha_n \cos[(n+1)T\omega] * \frac{1}{\omega - \omega_0} \cdot \\ \cdot \sum_{n=0}^{N-1} \alpha_n \cos[(n+1)T\omega] \quad (B-24)$$

$$I_3(\omega, \alpha_n) = P_\Omega(\omega) \frac{1/2}{\omega + \omega_0} \sum_{n=0}^{N-1} \alpha_n \cos[(n+1)T\omega] * \frac{1}{\omega - \omega_0} \cdot \\ \cdot \sum_{n=0}^{N-1} \alpha_n \cos(nT\omega) \quad (B-25)$$

$$I_4(\omega, \alpha_n) = P_\Omega(\omega) \frac{1/2}{\omega + \omega_0} \sum_{n=0}^{N-1} \alpha_n \cos(nT\omega) * \frac{1/2}{\omega - \omega_0} \cdot \\ \cdot \sum_{n=0}^{N-1} \alpha_n \cos[(n+1)T\omega] \quad (B-26)$$

The integrals $I_1(\omega, \alpha_n), \dots, I_4(\omega, \alpha_n)$ will be examined separately.

$$I_1(\omega, \alpha_n) = -\frac{1}{2} \int_{\omega_0 + \omega - \frac{\Omega}{2}}^{\omega_0 + \frac{\Omega}{2}} \left[\frac{1}{(\psi - \omega_0)(\omega - \psi + \omega_0)} \right] \sum_{n=0}^{N-1} \alpha_n \cos(nT\psi) \cdot \sum_{n=0}^{N-1} \alpha_n \cos[nT(\omega - \psi)] d\psi \quad 0 < \omega < \Omega \quad (\text{B-27})$$

$$-\frac{1}{4} \sum_{n=0}^{N-1} \sum_{k=0}^{N-1} \alpha_n \alpha_k \int_{\omega_0 + \omega - \frac{\Omega}{2}}^{\omega_0 + \frac{\Omega}{2}} \frac{\cos[(n-k)T\psi - kT\omega] + \cos[(n+k)T\psi - kT\omega]}{(\psi - \omega_0)(\omega - \psi + \omega_0)} d\psi. \quad (\text{B-28})$$

The expected value of $I_1(\omega, \alpha_n)$ is

$$I_1(\omega) = \mathcal{E}\{I_1(\omega, \alpha_n)\} \quad (\text{B-29})$$

$$= -\frac{1}{4} \sum_{n=0}^{N-1} \int_{\omega_0 + \omega - \frac{\Omega}{2}}^{\omega_0 + \frac{\Omega}{2}} \frac{\cos(nT\omega) + \cos(2nT\psi - nT\omega)}{(\psi - \omega_0)(\omega - \psi + \omega_0)} d\psi \quad (\text{B-30})$$

since

$$\mathcal{E}\{\alpha_n \alpha_k\} = \begin{cases} 0, & n \neq k \\ 1, & n = k \end{cases} \quad (\text{B-31})$$

An expansion of Equation (B-30) gives

$$I_1(\omega) = -\frac{1}{4} \sum_{n=0}^{N-1} \cos(nT\omega) \int_{\omega_0 + \omega - \frac{\Omega}{2}}^{\omega_0 + \frac{\Omega}{2}} \frac{d\psi}{(\psi - \omega_0)(\omega - \psi + \omega_0)} - \frac{1}{4} \sum_{n=0}^{N-1} \cos(nT\omega) \int_{\omega_0 + \omega - \frac{\Omega}{2}}^{\omega_0 + \frac{\Omega}{2}} \frac{\cos(2nT\psi)}{(\psi - \omega_0)(\omega - \psi + \omega_0)} d\psi - \frac{1}{4} \sum_{n=0}^{N-1} \sin(nT\omega) \int_{\omega_0 + \omega - \frac{\Omega}{2}}^{\omega_0 + \frac{\Omega}{2}} \frac{\sin(2nT\psi)}{(\psi - \omega_0)(\omega - \psi + \omega_0)} d\psi \quad (\text{B-32})$$

In a similar manner, the expected value of $I_2(\omega, \alpha_n)$ is

$$I_2(\omega) = \mathcal{E} \{I_2(\omega, \alpha_n)\} \quad (\text{B-33})$$

$$\begin{aligned} &= -\frac{1}{4} \sum_{n=0}^{N-1} \cos[(n+1)T\omega] \int_{\omega_0 + \omega - \frac{\Omega}{2}}^{\omega_0 + \frac{\Omega}{2}} \frac{d\psi}{(\psi - \omega_0)(\omega - \psi + \omega_0)} \\ &\quad - \frac{1}{4} \sum_{n=0}^{N-1} \cos[(n+1)T\omega] \int_{\omega_0 + \omega - \frac{\Omega}{2}}^{\omega_0 + \frac{\Omega}{2}} \frac{\cos[2(n+1)T\psi]}{(\psi - \omega_0)(\omega - \psi + \omega_0)} d\psi \\ &\quad - \frac{1}{4} \sum_{n=0}^{N-1} \sin[(n+1)T\omega] \int_{\omega_0 + \omega - \frac{\Omega}{2}}^{\omega_0 + \frac{\Omega}{2}} \frac{\sin[2(n+1)T\psi]}{(\psi - \omega_0)(\omega - \psi + \omega_0)} d\psi \quad 0 < \omega < \Omega \end{aligned} \quad (\text{B-34})$$

The third integral is

$$\begin{aligned} I_3(\omega, \alpha_n) &= \frac{1}{2} \int_{\omega_0 + \omega - \frac{\Omega}{2}}^{\omega_0 + \frac{\Omega}{2}} \frac{1}{(\psi - \omega_0)(\omega - \psi + \omega_0)} \sum_{n=0}^{N-1} \alpha_n \cos(nT\psi) \\ &\quad \cdot \sum_{n=0}^{N-1} \alpha_n \cos[(n+1)T(\omega - \psi)] d\psi \end{aligned} \quad (\text{B-35})$$

$$\begin{aligned} &= \frac{1}{4} \sum_{n=0}^{N-1} \sum_{k=0}^{N-1} \alpha_n \alpha_k \left\{ \int_{\omega_0 + \omega - \frac{\Omega}{2}}^{\omega_0 + \frac{\Omega}{2}} \frac{\cos[(k-n-1)T\psi + (n+1)T\omega]}{(\psi - \omega_0)(\omega - \psi + \omega_0)} d\psi \right. \\ &\quad \left. + \int_{\omega_0 + \omega - \frac{\Omega}{2}}^{\omega_0 + \frac{\Omega}{2}} \frac{\cos[(n+k+1)T\psi - (n+1)T\omega]}{(\psi - \omega_0)(\omega - \psi + \omega_0)} d\psi \right\} \end{aligned} \quad (\text{B-36})$$

The expected value of $I_3(\omega, \alpha_n)$ is, from Equation (B-31),

$$I_3(\omega) = \mathcal{O} \{I_3(\omega, \alpha_n)\} \quad (\text{B-37})$$

$$\begin{aligned} &= \frac{1}{4} \int_{\omega_0 + \omega - \frac{\Omega}{2}}^{\omega_0 + \frac{\Omega}{2}} \frac{1}{(\psi - \omega_0)(\omega - \psi + \omega_0)} \sum_{n=0}^{N-1} \cos [T\psi - (n+1)T\omega] d\psi \\ &+ \frac{1}{4} \int_{\omega_0 + \omega - \frac{\Omega}{2}}^{\omega_0 + \frac{\Omega}{2}} \frac{1}{(\psi - \omega_0)(\omega - \psi + \omega_0)} \sum_{n=0}^{N-1} \cos [(2n+1)T\psi - (n+1)T\psi] d\psi \end{aligned} \quad (\text{B-38})$$

In a similar manner, the expected value of $I_4(\omega, \alpha_n)$ is

$$I_4(\omega) = \mathcal{O} \{I_4(\omega, \alpha_n)\} \quad (\text{B-39})$$

$$\begin{aligned} &= \frac{1}{4} \int_{\omega_0 + \omega - \frac{\Omega}{2}}^{\omega_0 + \frac{\Omega}{2}} \frac{1}{(\psi - \omega_0)(\omega - \psi + \omega_0)} \sum_{n=0}^{N-1} \cos (T\alpha + nT\omega) \\ &+ \frac{1}{4} \int_{\omega_0 + \omega - \frac{\Omega}{2}}^{\omega_0 + \frac{\Omega}{2}} \frac{1}{(\psi - \omega_0)(\omega - \psi + \omega_0)} \sum_{n=0}^{N-1} \cos [(2n+1)T\alpha - nT\omega] d\psi \end{aligned} \quad (\text{B-40})$$

From Equation (B-22)

$$\mathcal{O} \{R_G(\omega, \alpha_n) * R_G(\omega, \alpha_n)\} = I_1(\omega) + I_2(\omega) + I_3(\omega) + I_4(\omega) \quad (\text{B-41})$$

As discussed previously, the derivation of $X_G(\omega, \alpha_n) * X_G(\omega, \alpha_n)$ will not be given here. However, the method is similar to that given for $R_G(\omega, \alpha_n) * R_G(\omega, \alpha_n)$. The results are

$$\begin{aligned}
& \int_{\omega_0 + \omega - \frac{\Omega}{2}}^{\omega_0 + \omega + \frac{\Omega}{2}} \frac{d\psi}{(\psi - \omega_0)(\omega - \psi + \omega_0)} \\
& - \frac{1}{4} \sum_{n=0}^{N-1} \cos(nT\omega) \int_{\omega_0 + \omega - \frac{\Omega}{2}}^{\omega_0 + \omega + \frac{\Omega}{2}} \frac{\cos(2nT\psi)}{(\psi - \omega_0)(\omega - \psi + \omega_0)} d\psi \\
& - \frac{1}{4} \sum_{n=0}^{N-1} \sin(nT\omega) \int_{\omega_0 + \omega - \frac{\Omega}{2}}^{\omega_0 + \omega + \frac{\Omega}{2}} \frac{\sin(2nT\psi)}{(\psi - \omega_0)(\omega - \psi + \omega_0)} d\psi \\
& + \frac{1}{4} \sum_{n=0}^{N-1} \sin[(n+1)T\omega] \int_{\omega_0 + \omega - \frac{\Omega}{2}}^{\omega_0 + \omega + \frac{\Omega}{2}} \frac{\sin[2(n+1)T\psi]}{(\psi - \omega_0)(\omega - \psi + \omega_0)} d\psi \\
& + \frac{1}{4} \int_{\omega_0 + \omega - \frac{\Omega}{2}}^{\omega_0 + \omega + \frac{\Omega}{2}} \frac{1}{(\psi - \omega_0)(\omega - \psi + \omega_0)} \sum_{n=0}^{N-1} \cos[(2n+1)T\psi - (n+1)T\omega] d\psi \\
& - \frac{1}{4} \int_{\omega_0 + \omega - \frac{\Omega}{2}}^{\omega_0 + \omega + \frac{\Omega}{2}} \frac{1}{(\psi - \omega_0)(\omega - \psi + \omega_0)} \sum_{n=0}^{N-1} \cos[T\psi - (n+1)T\omega] d\psi \\
& + \frac{1}{4} \int_{\omega_0 + \omega - \frac{\Omega}{2}}^{\omega_0 + \omega + \frac{\Omega}{2}} \frac{1}{(\psi - \omega_0)(\omega - \psi + \omega_0)} \sum_{n=0}^{N-1} \cos(2n+1)T\psi - [nT\omega] d\psi \\
& - \frac{1}{4} \int_{\omega_0 + \omega - \frac{\Omega}{2}}^{\omega_0 + \omega + \frac{\Omega}{2}} \frac{1}{(\psi - \omega_0)(\omega - \psi + \omega_0)} \sum_{n=0}^{N-1} \cos(T\psi + nT\omega) d\psi
\end{aligned} \tag{B-42}$$

From Equation (B-18), the expected value of $G_2(\omega, \alpha_n)$ is

$$G_2(\omega) = \mathcal{E}\{G_2(\omega, \alpha_n)\} \quad (B-43)$$

$$\begin{aligned} &= \frac{1}{2\pi} \mathcal{E}\{R_G(\omega, \alpha_n) * R_G(\omega, \alpha_n)\} \\ &\quad - \frac{1}{2\pi} \mathcal{E}\{X_G(\omega, \alpha_n) * X_G(\omega, \alpha_n)\} \end{aligned} \quad (B-44)$$

A combination of Equations (B-41), (B-42), and (B-44) give

$$\begin{aligned} G_2(\omega) &= -\frac{1}{4\pi} \sum_{n=0}^{N-1} \cos(nT\omega) \int_{\omega_0 + \omega - \frac{\Omega}{2}}^{\omega_0 + \frac{\Omega}{2}} \frac{d\psi}{(\psi - \omega_0)(\omega_0 - \psi + \omega_0)} \\ &\quad - \frac{1}{4\pi} \sum_{n=0}^{N-1} \cos[(n+1)T\omega] \int_{\omega_0 + \omega - \frac{\Omega}{2}}^{\omega_0 + \frac{\Omega}{2}} \frac{d\psi}{(\psi - \omega_0)(\omega_0 - \psi + \omega_0)} \\ &\quad + \frac{1}{4\pi} \int_{\omega_0 + \omega - \frac{\Omega}{2}}^{\omega_0 + \frac{\Omega}{2}} \frac{1}{(\psi - \omega_0)(\omega_0 - \psi + \omega_0)} \sum_{n=0}^{N-1} \cos[T\psi - (n+1)T\omega] d\psi \\ &\quad + \frac{1}{4\pi} \int_{\omega_0 + \omega - \frac{\Omega}{2}}^{\omega_0 + \frac{\Omega}{2}} \frac{1}{(\psi - \omega_0)(\omega_0 - \psi + \omega_0)} \sum_{n=0}^{N-1} \cos(T\psi + nT\omega) d\psi \end{aligned} \quad (B-45)$$

Collecting terms and simplifying in Equation (B-45)

$$\begin{aligned}
 G_2(\omega) = & -\frac{1}{4\pi} \left[1 + \cos(NT\omega) + 2 \sum_{n=0}^{N-1} \cos(nT\omega) \right] \cdot \\
 & \int_{\omega_0 + \omega - \frac{\Omega}{2}}^{\omega_0 + \frac{\Omega}{2}} \frac{d\psi}{(\psi - \omega_0)(\omega - \psi + \omega_0)} - \int_{\omega_0 + \omega - \frac{\Omega}{2}}^{\omega_0 + \frac{\Omega}{2}} \frac{\cos(T\psi)}{(\psi - \omega_0)(\omega - \psi + \omega_0)} d\psi \\
 & + \frac{1}{4\pi} \sin(NT\omega) \int_{\omega_0 + \omega - \frac{\Omega}{2}}^{\omega_0 + \frac{\Omega}{2}} \frac{\sin(T\psi)}{(\psi - \omega_0)(\omega - \psi + \omega_0)} d\psi \quad 0 \leq \omega \leq \Omega
 \end{aligned} \tag{B-46}$$

The three integrals in Equation (B-46) may be further simplified. The results are

$$\int_{\omega_0 + \omega - \frac{\Omega}{2}}^{\omega_0 + \frac{\Omega}{2}} \frac{d\psi}{(\psi - \omega_0)(\omega - \psi + \omega_0)} = -\frac{2}{\omega} \left\{ \ln(T|\omega - \frac{\Omega}{2}|) - \ln(\frac{T\Omega}{2}) \right\} \quad 0 \leq \omega \leq \Omega \tag{B-47}$$

$$\int_{\omega_0 + \omega - \frac{\Omega}{2}}^{\omega_0 + \frac{\Omega}{2}} \frac{\cos(T\psi)}{(\psi - \omega_0)(\omega - \psi + \omega_0)} d\psi = \left[\frac{1 + \cos(T\omega)}{\omega} \right] \left\{ \int_{\infty}^{\frac{T\Omega}{2}} \frac{\cos(t)}{t} dt - \int_{\infty}^{T|\omega - \frac{\Omega}{2}|} \frac{\cos(t)}{t} dt \right\} \tag{B-48}$$

$$= \left[\frac{1 + \cos(T\omega)}{\omega} \right] \left[C_i\left(\frac{T\Omega}{2}\right) - C_i\left(T|\omega - \frac{\Omega}{2}|\right) \right] \quad 0 \leq \omega \leq \Omega \tag{B-49}$$

where $C_i(x)$ is the cosine integral shown in Figure B-1.

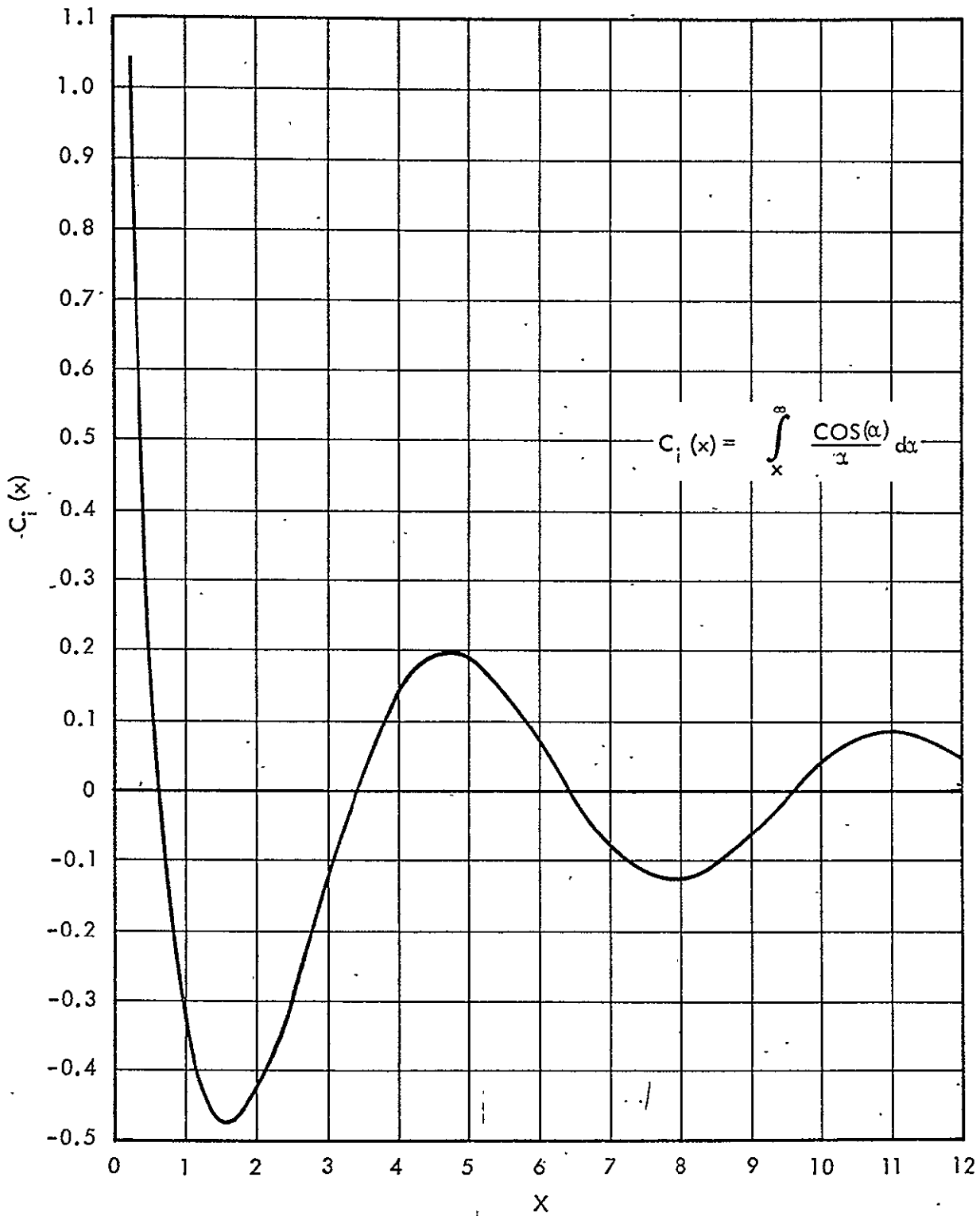


Figure B-4. The Cosine Integral

The third integral in Equation (B-46) is

$$\begin{aligned}
 \int_{\omega_0 + \omega - \frac{\Omega}{2}}^{\omega_0 + \frac{\Omega}{2}} \frac{\sin(T\psi)}{(\psi - \omega_0)(\omega - \psi + \omega_0)} d\psi &= \left[\frac{1 - \cos(T\omega)}{\omega} \right] \left\{ \int_0^{\frac{T\Omega}{2}} \frac{\sin(t)}{t} dt \right. \\
 &\quad \left. - \int_0^{T(\omega - \frac{\Omega}{2})} \frac{\sin(t)}{t} dt \right\} \\
 &\quad + \frac{\sin(T\omega)}{\omega} \left\{ \int_{\infty}^{\frac{T\Omega}{2}} \frac{\cos(t)}{t} dt \right. \\
 &\quad \left. - \int_0^{T(\omega - \frac{\Omega}{2})} \frac{\cos(t)}{t} dt \right\} \quad (B-50)
 \end{aligned}$$

$$\begin{aligned}
 &\left[\frac{1 - \cos(T\omega)}{\omega} \right] \left[S_i\left(\frac{T\Omega}{2}\right) - S_i\left(T\left(\omega - \frac{\Omega}{2}\right)\right) \right] \\
 &+ \frac{\sin(T\omega)}{\omega} \left[C_i\left(\frac{T\Omega}{2}\right) - C_i\left(T\left|\omega - \frac{\Omega}{2}\right|\right) \right] \quad 0 \leq \omega \leq \Omega \quad (B-51)
 \end{aligned}$$

where $S_i(x)$ is the sine integral.

The substitution of Equation (B-47), (B-49), and (B-51) into Equation (B-46), and rearranging terms gives

$$\begin{aligned}
 G_2(\omega) &= \frac{1}{2\pi\omega} \left[1 + \cos(NT\omega) + 2 \sum_{n=1}^{N-1} \cos(nT\omega) \right] \left[\ln\left(T\left|\omega - \frac{\Omega}{2}\right|\right) \right. \\
 &\quad \left. - C_i\left(T\left|\omega - \frac{\Omega}{2}\right|\right) - \ln\left(\frac{T\Omega}{2}\right) + C_i\left(\frac{T\Omega}{2}\right) \right] + \frac{\sin(NT\omega)}{2\pi\omega} \left[S_i\left(\frac{T\Omega}{2}\right) \right. \\
 &\quad \left. - S_i\left(T\left(\omega - \frac{\Omega}{2}\right)\right) \right] \quad 0 \leq \omega \leq \Omega \quad (B-52)
 \end{aligned}$$

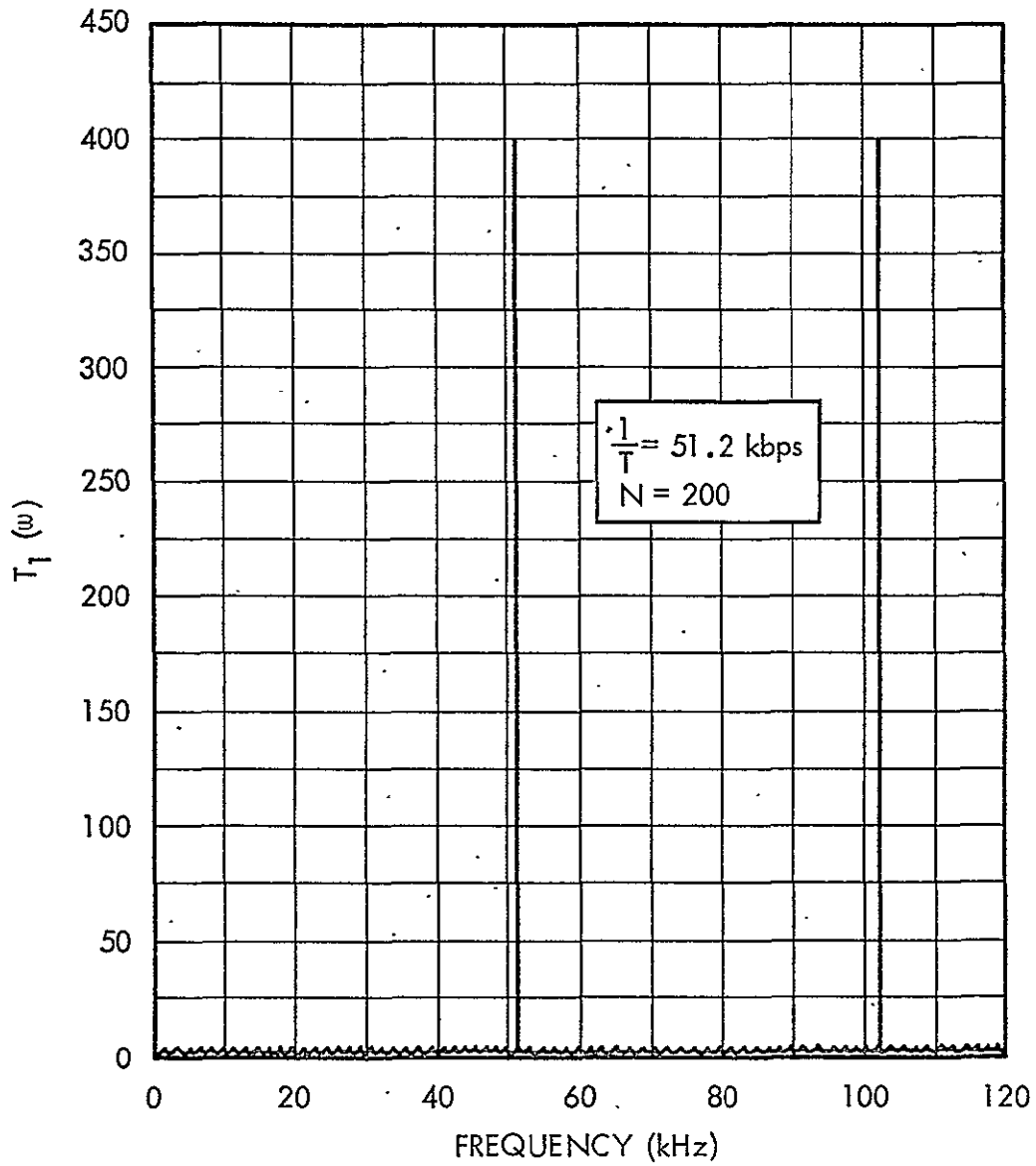


Figure B-2. $T_1(\omega)$ versus Frequency

The terms in Equation (B-52) will be examined individually. The first term is

$$T_1(\omega) = 1 + \cos(NT\omega) + 2 \sum_{n=1}^{N-1} \cos(nT\omega) \quad (\text{B-53})$$

Recall the Fourier Series expansion

$$\frac{\pi}{T} \sum_{n=-\infty}^{\infty} \delta\left[\omega + n\left(\frac{2\pi}{T}\right)\right] = 1 + \sum_{n=1}^{\infty} \cos(nT\omega) \quad (\text{B-54})$$

where $\delta(\omega)$ is the Dirac delta function. For large N , Equation (B-46) becomes

$$\begin{aligned} \lim_{N \rightarrow \infty} \left\{ 1 + \cos(NT\omega) + 2 \sum_{n=1}^{N-1} \cos(nT\omega) \right\} &= \cos(NT\omega) - 1 \\ &+ \frac{2\pi}{T} \sum_{n=-\infty}^{\infty} \delta\left[\omega - n\left(\frac{2\pi}{T}\right)\right] \end{aligned} \quad (\text{B-55})$$

Equation (B-55) indicates that as N becomes large, $T_1(\omega)$ approaches a series of impulse functions located at integral multiples of $\frac{2\pi}{T}$. For finite values of N ,

$$1 + \cos(NT\omega) + 2 \sum_{n=1}^{N-1} \cos(nT\omega) \Bigg|_{\omega = 0, \frac{2\pi}{T}, \frac{4\pi}{T}, \dots} = 2N \quad (\text{B-56})$$

A plot of $T_1(\omega)$ is shown in Figure B-2.

The second term in Equation (B-52) is

$$T_2(\omega) = \frac{1}{\omega} \left[\ln\left(T\left|\omega - \frac{\Omega}{2}\right|\right) - C_1\left(T\left|\omega - \frac{\Omega}{2}\right|\right) - \ln\left(\frac{T\Omega}{2}\right) + C_1\left(\frac{T\Omega}{2}\right) \right] \quad (\text{B-57})$$

It may be shown that

$$\lim_{\omega \rightarrow \frac{\Omega}{2}} \left\{ T_2(\omega) \right\} = \frac{2}{\Omega} \left[-\gamma - \ln \left(\frac{T\Omega}{2} \right) + C_i \left(\frac{T\Omega}{2} \right) \right] \quad (\text{B-58})$$

where γ is Euler's constant

$$\gamma = 0.5772156649. . . \quad (\text{B-59})$$

It may also be shown that

$$\lim_{\omega \rightarrow 0} \left\{ T_2(\omega) \right\} = \frac{2}{\Omega} \left[\cos \left(\frac{T\Omega}{2} \right) - 1 \right] \quad (\text{B-60})$$

The last term in Equation (B-52) is

$$T_3(\omega) = \frac{\sin(NT\omega)}{\omega} \left[S_i \left(\frac{T\Omega}{2} \right) - S_i \left[T \left(\omega - \frac{\Omega}{2} \right) \right] \right] \quad (\text{B-61})$$

The limit as ω approaches zero is

$$\lim_{\omega \rightarrow 0} \left\{ T_3(\omega) \right\} = 2NT \left[S_i \left(\frac{T\Omega}{2} \right) \right] \quad (\text{B-62})$$

and

$$T_3(\omega) \Big|_{\omega = \frac{2\pi}{T}, \frac{4\pi}{T}, \dots} = 0 \quad (\text{B-63})$$

The results of the preceding analysis are best summarized by referring back to Equation (B-52). The series of spurs in $T_1(\omega)$ are "amplitude modulated" by the "envelope function" $T_2(\omega)$. If the subcarrier filter bandwidth is changed, there is a corresponding change in the relative spur magnitudes. It is important to note that the largest spur will always occur near one-half the subcarrier filter bandwidth.

The amplitude spectrum of $e(t, \alpha_n)$ is, from Equation (B-5),

$$A(\omega, \alpha_n) = \left| A \mathcal{F} \left\{ \sin(\omega_c t) \right\} - \frac{A a \beta^2}{2\pi} \mathcal{F} \left\{ \sin(\omega_c t) \right\} * G_2(\omega, \alpha_n) \right. \\ \left. + \frac{A \beta}{2\pi} \mathcal{F} \left\{ \cos(\omega_c t) \right\} * G(\omega, \alpha_n) \right| \quad (\text{B-64})$$

$$A(\omega, \alpha_n) = \begin{cases} \left| -\frac{ANT}{2} + \frac{A a \beta^2}{2} G_2(0, \alpha_n) \right| & \omega = \omega_c \\ \left| \frac{A a \beta^2}{2} G_2(\omega - \omega_c, \alpha_n) \right| & \omega = \omega_c + K \left(\frac{2\pi}{T} \right), k=1, 2, \dots \\ \left| \frac{A \beta}{\pi} G(\omega - \omega_c, \alpha_n) \right| & \omega \text{ near } \omega_o \end{cases} \quad (\text{B-65})$$

The expected value of $A(\omega, \alpha_n)$ is

$$A(\omega) = \mathcal{E} \left\{ A(\omega, \alpha_n) \right\} \quad (\text{B-66})$$

$$= \begin{cases} \frac{A}{2} \left[NT - a \beta^2 G_2(0) \right] & \omega = \omega_c \\ -\frac{A a \beta^2}{2} G_2(\omega - \omega_c) & \omega = \omega_c + k \left(\frac{2\pi}{T} \right), k=1, 2, \dots \\ \mathcal{E} \left\{ \left| \frac{A \beta}{\pi} G(\omega - \omega_c, \alpha_n) \right| \right\} & \omega \text{ near } \omega_o \end{cases} \quad (\text{B-67})$$

Thus, from Equations (B-52), (B-56), (B-60), (B-62), and (B-67)

$$A(\omega) = \begin{cases} \frac{ANT}{2} \left\{ 1 - \frac{a \beta^2}{\pi} \left(S_i \left(\frac{T\Omega}{2} \right) - \frac{2}{\Omega T} \left[1 - \cos \left(\frac{T\Omega}{2} \right) \right] \right) \right\} & \omega = \omega_c \\ -\frac{ANa \beta^2}{2\pi} \left(\frac{1}{\omega_d} \right) \left[\ln \left(T \left| \omega_d - \frac{\Omega}{2} \right| \right) - C_i \left(T \left| \omega_d - \frac{\Omega}{2} \right| \right) \right. \\ \left. - \ln \left(\frac{T\Omega}{2} \right) + C_i \left(\frac{T\Omega}{2} \right) \right] & \omega_d = k \left(\frac{2\pi}{T} \right), k=1, 2, \dots \\ \mathcal{E} \left\{ \left| \frac{A \beta}{\pi} G(\omega_d, \alpha_n) \right| \right\} & \omega \text{ near } \omega_o \end{cases} \quad (\text{B-68})$$

where ω_d is the distance away from the carrier radian frequency ω_c

$$\omega_d = \omega - \omega_c \quad (B-69)$$

The ratio (in dB) of the kth spur magnitude to the carrier magnitude is, from Equation (B-68),

$$R_{dB}(k, \Omega, \beta, T) = 20 \log_{10} \left\{ \frac{-a}{2k} \left(\frac{\beta}{\pi} \right)^2 \left[\frac{\ln \left(\left| 2\pi k - \frac{T\Omega}{2} \right| \right) - C_1 \left(\left| 2\pi k - \frac{T\Omega}{2} \right| \right) - \ln \left(\frac{T\Omega}{2} \right) + C_1 \left(\frac{T\Omega}{2} \right)}{1 - \frac{a\beta^2}{\pi} \left[S_i \left(\frac{T\Omega}{2} \right) - \frac{2}{T\Omega} \left(1 - \cos \left(\frac{T\Omega}{2} \right) \right) \right]} \right] \right\} \quad (B-70)$$

where

$$\text{Location of the kth spur} = \omega_c \pm k \left(\frac{2\pi}{T} \right) \quad (B-71)$$

APPENDIX C

AMPLITUDE DISTORTION IN THE BAND-LIMITED, BIPHASE MODULATED SUBCARRIER

The unfiltered biphas modulated subcarrier is discussed in detail in Appendix A. From Equation (A-5),

$$f(t) = m'(t) \sin(\omega_0 t) \quad (C-1)$$

where ω_0 is the subcarrier radian frequency, and

$$m'(t) = \begin{cases} 1, & \text{if the PCM-NRZ bit is 1} \\ -1, & \text{if the PCM-NRZ bit is 0} \end{cases} \quad (C-2)$$

The modulating function $m'(t)$ is a series of pulses having width T , $2T$, $3T$, etc., as shown in Figure C-1. The function $m'(t)$ may be considered to be the sum of a series of functions ($m_1(t)$, $m_2(t)$, ...) as illustrated in Figure C-1.

If $f(t)$ is band-limited by an ideal band-pass filter centered at ω_0 with bandwidth Ω , the output of the filter will be

$$f_\Omega(t) = m'_\Omega(t) \sin(\omega_0 t) \quad (C-3)$$

where $m'_\Omega(t)$ is the filtered version of $m'(t)$. Since $m'(t)$ is the sum of the functions $m_1(t)$, $m_2(t)$, ..., then $m'_\Omega(t)$ will be the sum of $m_{1\Omega}(t)$, $m_{2\Omega}(t)$, ..., where $m_{n\Omega}(t)$ is the filtered version of $m_n(t)$.

An expression for $m_{n\Omega}(t)$ may be obtained by referring to Figure C-2.

$$m_{n\Omega}(t) = \frac{1}{2\pi} \int_{-\frac{\Omega}{2}}^{\frac{\Omega}{2}} \left[\int_{-\infty}^{\infty} m_n(\alpha) e^{-j\omega\alpha} d\alpha \right] e^{j\omega t} d\omega \quad (C-4)$$

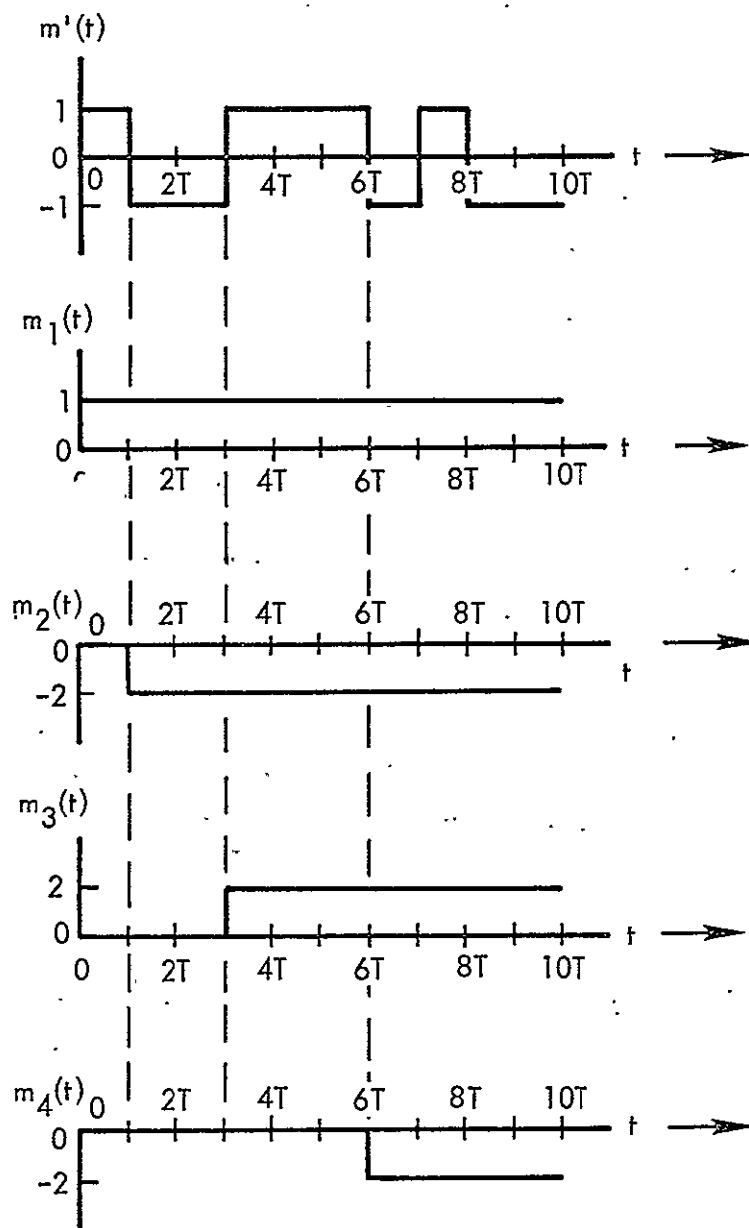


Figure C-1. Modulating Function Expressed as the Sum of a Series of Step Functions

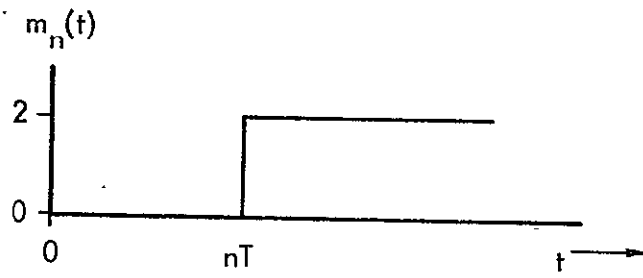


Figure C-2. Basic Step Function

$$m_n^\Omega(t) = \frac{1}{2\pi} \int_{-\infty}^{\infty} m_n(\alpha) \int_{-\frac{\Omega}{2}}^{\frac{\Omega}{2}} e^{j\omega(t-\alpha)} d\omega d\alpha \quad (C-5)$$

$$= \frac{2}{\pi} \int_{nT}^{\infty} \frac{\sin[\Omega(t-\alpha)]}{t-\alpha} d\alpha \quad n \neq 1 \quad (C-6)$$

$$= -\frac{2}{\pi} \int_{\frac{\Omega}{2}(t-nT)}^{-\infty} \frac{\sin(x)}{x} dx \quad n \neq 1 \quad (C-7)$$

$$= 1 + \frac{2}{\pi} S_i \left[\frac{\Omega}{2}(t-nT) \right] \quad n \neq 1 \quad (C-8)$$

A plot of Equation (C-8) is illustrated in Figure C-3. If a "1" bit is followed by a "0" bit, the filtered wave shape will be

$$f_\Omega(1, 0) = \frac{2}{\pi} \left\{ S_i \left[\frac{\Omega}{2}(t-nT) \right] - S_i \left[\frac{\Omega}{2}(t-nT + T) \right] \right\} \quad (C-9)$$

Equation (C-8) is illustrated in Figure C-4. From Equation C-1 it can be seen that the subcarrier will be amplitude modulated by a wave shape similar to that shown in Figure C-4.

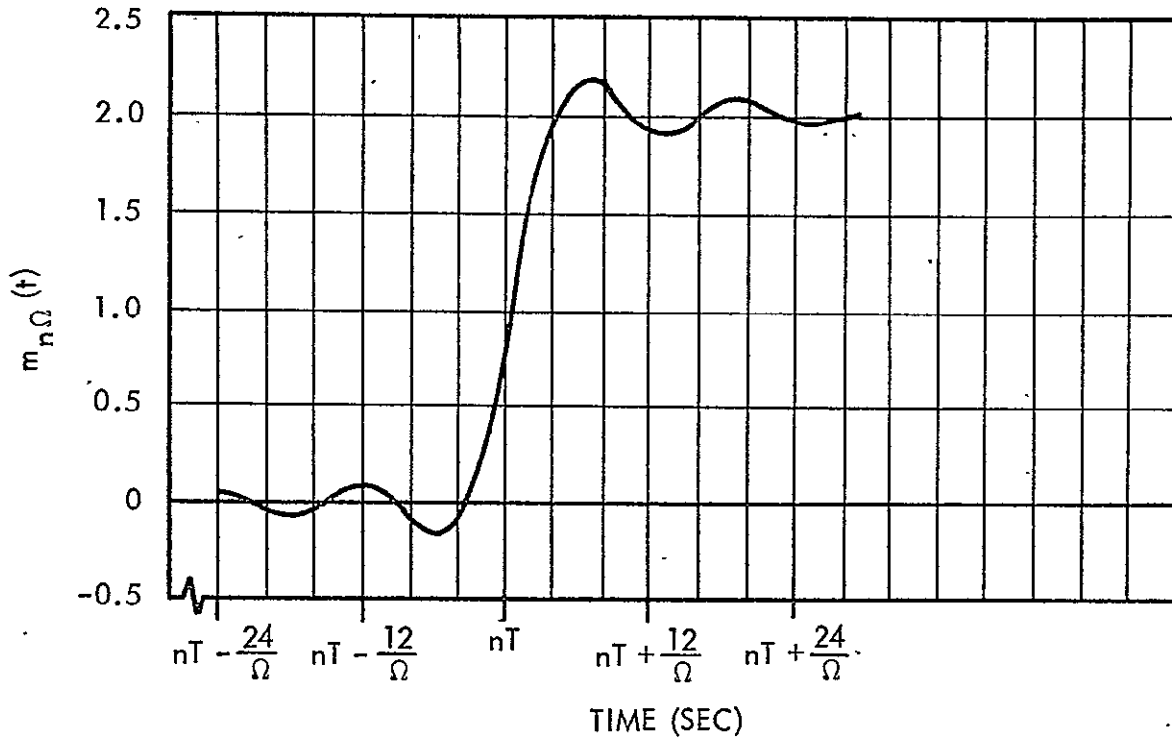


Figure C-3. Filtered Step Function (Equation (C-8))

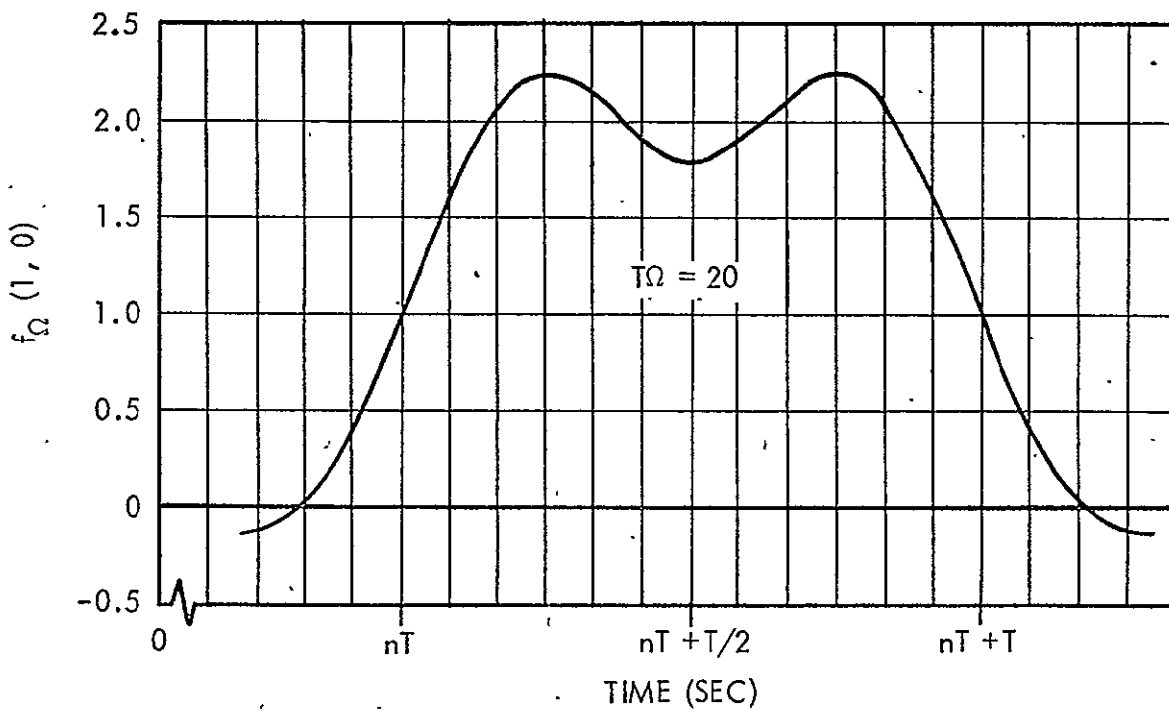


Figure C-4. Filtered Time Function Resulting from a Bit Change

APPENDIX D

THE APPROXIMATION OF $\cos [\beta g(t)]$

The power series expansion of $\cos [\beta g(t)]$ is

$$\cos [\beta g(t)] = 1 - \frac{\beta^2 g^2(t)}{2!} + \frac{\beta^4 g^4(t)}{4!} - \dots \quad (D-1)$$

The desired approximation in the interval $-1.5 \leq \beta g(t) \leq 1.5$ is

$$\cos [\beta g(t)] \cong 1 - a\beta^2 g^2(t), \quad (D-2)$$

where a is chosen to minimize the mean square error.

The square error is given by

$$\mathcal{E} [a, \beta g(t)] = \left[\cos[\beta g(t)] - 1 + a\beta^2 g^2(t) \right]^2 \quad (D-3)$$

The mean of $\mathcal{E} [a, \beta g(t)]$ is

$$\mathcal{E}(a) = \frac{2}{1.5} \int_0^{1.5} \left[\cos[\beta g(t)] - 1 + a\beta^2 g^2(t) \right]^2 d[\beta g(t)] \quad (D-4)$$

$$= \frac{2}{1.5} \int_0^{1.5} \left[\cos(x) - 1 + ax^2 \right]^2 dx \quad (D-5)$$

The value of a which minimizes $\mathcal{E}(a)$ is the solution to

$$\frac{d\mathcal{E}(a)}{da} = 0 \quad (D-6)$$

$$\int_0^{1.5} x^2 \left[\cos(x) - 1 + ax^2 \right] dx = 0 \quad (D-7)$$

The value of a which satisfies Equation (D-6) is

$$a = 0.4368 \quad (D-7)$$

It is shown in Appendix C that, approximately

$$-1 \leq g(t) \leq 1$$

Then

$$-1.5 \leq \beta g(t) \leq 1.5 \quad (D-8)$$

implies that

$$0 \leq \beta \leq 1.5 \quad (D-9)$$

Thus,

$$\cos [\beta g(t)] \cong 1 - (0.4368)\beta g^2(t), \quad 0 \leq \beta \leq 1.5 \quad (D-10)$$

which is the desired approximation. The approximation is plotted with $\cos(X)$ in Figure D-1.

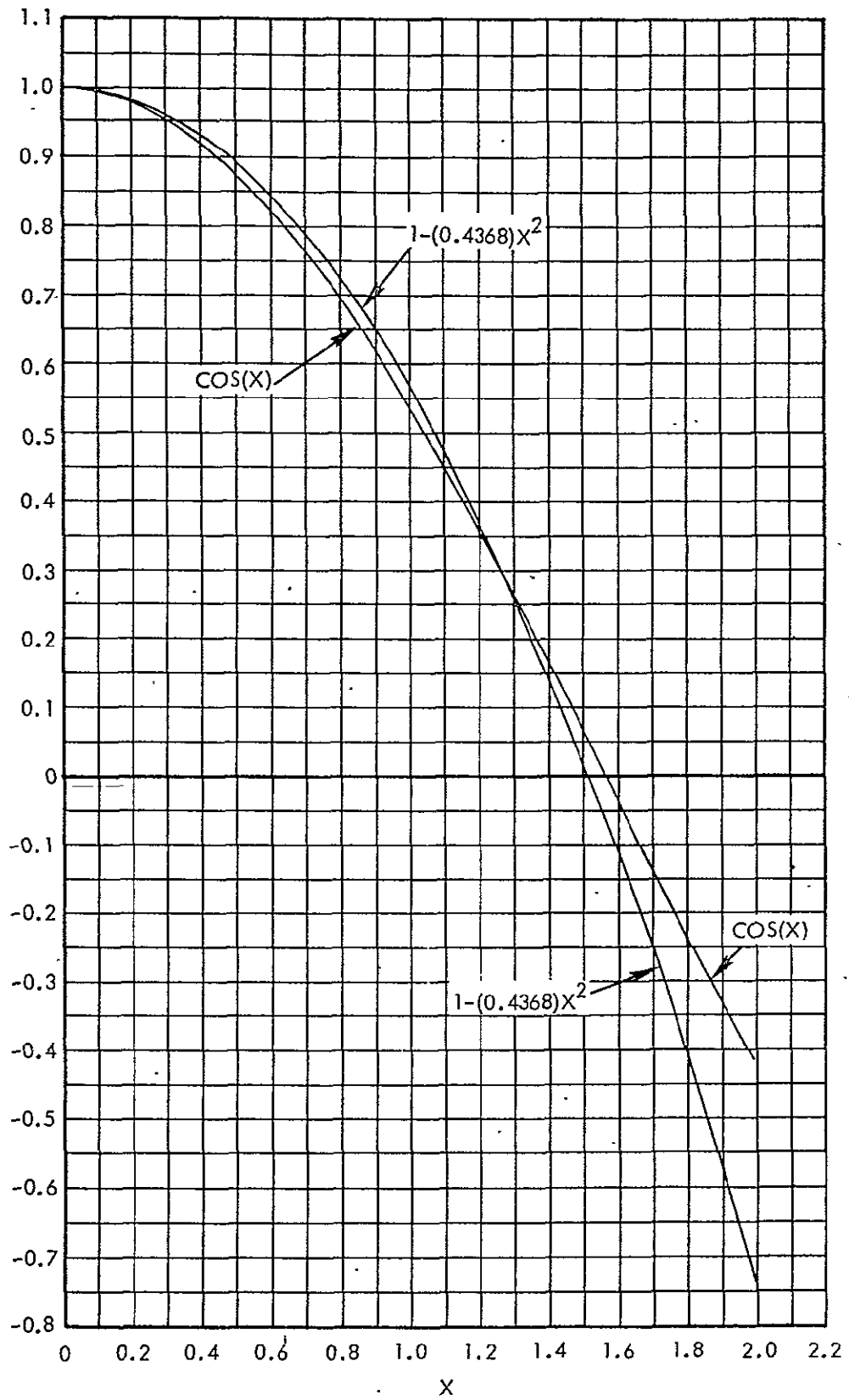


Figure D-1. Cos(X) and Its Approximation for Values of X Less Than or Equal to 1.5

APPENDIX E

THE SPECTRAL DENSITY OF A SINUSOID PHASE MODULATED BY A TIME-LIMITED, APERIODIC PCM-NRZ CODE

The Fourier transform of a sinusoid phase modulated by a time limited aperiodic PCM-NRZ code has been derived previously, Equation A-26, and is repeated here.

$$F(\omega, \alpha_n) = \mathcal{F}\{f(t, \alpha_n)\} \quad (\text{E-1})$$

$$= 2(-1)^{k+1} \sin\left(\frac{\omega T}{2}\right) \left[\frac{\omega_0}{\omega^2 - \omega_0^2} \right] \cdot$$

$$\left[\sum_{n=0}^{N-1} \alpha_n \sin\left(n + \frac{1}{2}\right)T\omega + j \sum_{n=0}^{N-1} \alpha_n \cos\left(n + \frac{1}{2}\right)T\omega \right] \quad (\text{E-2})$$

The quantities $f(t, \alpha_n)$ and $F(\omega, \alpha_n)$ are both stochastic processes in that they represent an ensemble of functions, each of which is uniquely determined by the sequence of α_n 's. That is, for any given PCM-NRZ bit sequence, there is determined a unique $f(t)$ and $F(\omega)$.

The "average random power" of the process $f(t, \alpha_n)$ in the interval $(0, T')$ is

$$S_{NT}(\omega, \alpha_n) = \frac{1}{T'} \left| \int_0^{T'} f(t, \alpha_n) e^{-j\omega t} dt \right|^2 \quad (\text{E-3})$$

where

$$T' = \text{time duration of } f(t, \alpha_n) \quad (\text{E-4})$$

$$= NT \quad (\text{E-5})$$

Thus,

$$S_{NT}(\omega, \alpha_n) = \frac{1}{NT} \left| \int_0^{NT} f(t, \alpha_n) e^{-j\omega t} dt \right|^2 \quad (E-6)$$

But

$$\int_0^{NT} f(t, \alpha_n) e^{-j\omega t} dt = F(\omega, \alpha_n) \quad (E-7)$$

Thus,

$$S_{NT}(\omega, \alpha_n) = \frac{1}{NT} \left| F(\omega, \alpha_n) \right|^2 \quad (E-8)$$

$$= \frac{1}{NT} \left| 2(-1)^{k+1} \sin \left(\frac{\omega T}{2} \right) \left[\frac{\omega_0}{\omega^2 - \omega_0^2} \right] \left\{ \sum_{n=0}^{N-1} \alpha_n \sin \left[(n + \frac{1}{2})T\omega \right] \right. \right. \\ \left. \left. + j \sum_{n=0}^{N-1} \alpha_n \cos \left[(n + \frac{1}{2})T\omega \right] \right\} \right|^2 \quad (E-9)$$

$$= \frac{T}{2N} \left[\frac{\sin \frac{T\omega}{2}}{(\omega - \omega_0)T/2} \right]^2 \left[\frac{1}{\frac{\omega}{\omega_0} + 1} \right]^2 \left| \sum_{n=0}^{N-1} \alpha_n \sin \left[(n + \frac{1}{2})T\omega \right] \right.$$

$$\left. + j \sum_{n=0}^{N-1} \alpha_n \cos \left[(n + \frac{1}{2})T\omega \right] \right|^2 \quad (E-10)$$

Let

$$A(\omega, \alpha_n) = \left| \sum_{n=0}^{N-1} \alpha_n \sin \left[\left(n + \frac{1}{2} \right) T\omega \right] + j \sum_{n=0}^{N-1} \alpha_n \cos \left[\left(n + \frac{1}{2} \right) T\omega \right] \right|^2 \quad (\text{E-11})$$

$$= \left\{ \sum_{n=0}^{N-1} \alpha_n \cos \left[\left(n + \frac{1}{2} \right) T\omega \right] \right\}^2 + \left\{ \sum_{n=0}^{N-1} \alpha_n \sin \left[\left(n + \frac{1}{2} \right) T\omega \right] \right\}^2 \quad (\text{E-12})$$

$$\sum_{n=0}^{N-1} \alpha_n^2 \cos^2 \left[\left(n + \frac{1}{2} \right) T\omega \right] + \sum_{n=0}^{N-1} \alpha_n^2 \sin^2 \left[\left(n + \frac{1}{2} \right) T\omega \right]$$

$$+ 2\alpha_0 \cos \left(\frac{T\omega}{2} \right) \sum_{n=1}^{N-1} \alpha_n \cos \left[\left(n + \frac{1}{2} \right) T\omega \right]$$

$$+ 2\alpha_1 \cos \left(\frac{3T\omega}{2} \right) \sum_{n=2}^{N-1} \alpha_n \cos \left[\left(n + \frac{1}{2} \right) T\omega \right]$$

$$+ 2\alpha_2 \cos \left(\frac{5T\omega}{2} \right) \sum_{n=3}^{N-1} \alpha_n \cos \left[\left(n + \frac{1}{2} \right) T\omega \right]$$

$$+ \dots + 2\alpha_{N-2} \alpha_{N-1} \cos \left[\left(N - \frac{3}{2} \right) T\omega \right] \cos \left[\left(N - \frac{1}{2} \right) T\omega \right]$$

$$+ 2\alpha_0 \sin \left(\frac{T\omega}{2} \right) \sum_{n=1}^{N-1} \alpha_n \sin \left[\left(n + \frac{1}{2} \right) T\omega \right]$$

$$+ 2\alpha_1 \sin \left(\frac{3T\omega}{2} \right) \sum_{n=2}^{N-1} \alpha_n \sin \left[\left(n + \frac{1}{2} \right) T\omega \right]$$

$$\begin{aligned}
& + 2\alpha_2 \sin\left(\frac{5T\omega}{2}\right) \sum_{n=3}^{N-1} \alpha_n \sin\left[\left(n + \frac{1}{2}\right)T\omega\right] \\
& + \dots + 2\alpha_{N-2} \alpha_{N-1} \sin\left[\left(N - \frac{3}{2}\right)T\omega\right] \sin\left[\left(N - \frac{1}{2}\right)T\omega\right] \quad (\text{E-13})
\end{aligned}$$

$$\begin{aligned}
A(\omega, \alpha_n) = & N + 2\alpha_0 \left\{ \cos\left(\frac{T\omega}{2}\right) \sum_{n=1}^{N-1} \alpha_n \cos\left[\left(n + \frac{1}{2}\right)T\omega\right] \right. \\
& \left. + \sin\left(\frac{T\omega}{2}\right) \sum_{n=1}^{N-1} \alpha_n \sin\left[\left(n + \frac{1}{2}\right)T\omega\right] \right\} \\
& + 2\alpha_1 \left\{ \cos\left(\frac{3T\omega}{2}\right) \sum_{n=2}^{N-1} \alpha_n \cos\left[\left(n + \frac{1}{2}\right)T\omega\right] \right. \\
& \left. + \sin\left(\frac{3T\omega}{2}\right) \sum_{n=2}^{N-1} \alpha_n \sin\left[\left(n + \frac{1}{2}\right)T\omega\right] \right\} \\
& + 2\alpha_2 \left\{ \cos\left(\frac{5T\omega}{2}\right) \sum_{n=3}^{N-1} \alpha_n \cos\left[\left(n + \frac{1}{2}\right)T\omega\right] \right. \\
& \left. + \sin\left(\frac{5T\omega}{2}\right) \sum_{n=3}^{N-1} \alpha_n \sin\left[\left(n + \frac{1}{2}\right)T\omega\right] \right\} \\
& + \dots + 2\alpha_{N-2} \left\{ \alpha_{N-1} \cos\left[\left(N - \frac{3}{2}\right)T\omega\right] \cos\left[\left(N - \frac{1}{2}\right)T\omega\right] \right. \\
& \left. + \alpha_{N-1} \sin\left[\left(N - \frac{3}{2}\right)T\omega\right] \sin\left[\left(N - \frac{1}{2}\right)T\omega\right] \right\} \quad (\text{E-14})
\end{aligned}$$

$$\begin{aligned}
A(\omega, \alpha_n) &= N + 2\alpha_0 \sum_{n=1}^{N-1} \alpha_n \cos(nT\omega) + 2\alpha_1 \sum_{n=2}^{N-1} \alpha_n \cos[(n-1)T\omega] \\
&\quad + 2\alpha_2 \sum_{n=3}^{N-1} \alpha_n \cos[(n-2)T\omega] \\
&\quad + \dots + 2\alpha_{N-2} \alpha_{N-1} \cos(T\omega)
\end{aligned} \tag{E-15}$$

$$\begin{aligned}
&= N + 2 \cos(T\omega) \left\{ \alpha_0 \alpha_1 + \alpha_1 \alpha_2 + \alpha_2 \alpha_3 + \dots + \alpha_{N-2} \alpha_{N-1} \right\} \\
&\quad + 2 \cos(2T\omega) \left\{ \alpha_0 \alpha_2 + \alpha_1 \alpha_3 + \alpha_2 \alpha_4 + \dots + \alpha_{N-3} \alpha_{N-1} \right\} \\
&\quad + 2 \cos(3T\omega) \left\{ \alpha_0 \alpha_3 + \alpha_1 \alpha_4 + \alpha_2 \alpha_5 + \dots + \alpha_{N-4} \alpha_{N-1} \right\} \\
&\quad + \dots + 2 \cos[(N-1)T\omega] \left\{ \alpha_0 \alpha_{N-1} \right\}
\end{aligned} \tag{E-16}$$

$$= N + 2 \sum_{n=1}^{N-1} \gamma_n \cos(nT\omega) \tag{E-17}$$

where

$$\gamma_n = \sum_{k=0}^{N-1-n} \alpha_k \alpha_{k+n}, \quad n = 1, 2, 3, \dots, N-1 \tag{E-18}$$

Note that γ_n is a random variable depending on the α_n 's.

Thus, from Equations (E-10) and (E-17), the random process $S_{NT}(\omega, \alpha_n)$ is

$$S_{NT}(\omega, \alpha_n) = \frac{T}{2N} \left[\frac{\sin\left(\frac{\omega T}{2}\right)}{(\omega - \omega_0)T/2} \right]^2 \left[\frac{1}{\frac{\omega}{\omega_0} + 1} \right]^2 \left[N + 2 \sum_{n=1}^{N-1} \gamma_n \cos(nT\omega) \right] \tag{E-19}$$

The expected value of $S_{NT}(\omega, \alpha_n)$ is

$$\mathcal{E}\left\{S_{NT}(\omega, \alpha_n)\right\} = \frac{T}{2N} \left[\frac{\sin\left(\frac{\omega T}{2}\right)}{(\omega - \omega_0)T/2} \right]^2 \left[\frac{1}{\frac{\omega}{\omega_0} + 1} \right]^2 \left[N + 2 \sum_{n=1}^{N-1} \mathcal{E}\left\{\gamma_n\right\} \cos(nT\omega) \right] \quad (\text{E-20})$$

But, as is shown later

$$\mathcal{E}\left\{\gamma_n\right\} = 0. \quad (\text{E-21})$$

Thus,

$$\mathcal{E}\left\{S_{NT}(\omega, \alpha_n)\right\} = \frac{T}{2} \left[\frac{\sin\left(\frac{\omega T}{2}\right)}{(\omega - \omega_0)T/2} \right]^2 \left[\frac{1}{\frac{\omega}{\omega_0} + 1} \right]^2 \quad (\text{E-22})$$

Note that Equation (E-22) implies that $S_{NT}(\omega, \alpha_n)$ is nonstationary.

The variance of the process $S_{NT}(\omega, \alpha_n)$ may be computed using the results of Equation (E-22).

$$V(\omega) = \text{Variance of } S_{NT}(\omega, \alpha_n) \quad (\text{E-23})$$

$$= \mathcal{E}\left\{\left[S_{NT}(\omega, \alpha_n) - \mathcal{E}\left\{S_{NT}(\omega, \alpha_n)\right\}\right]^2\right\} \quad (\text{E-24})$$

$$= \mathcal{E}\left\{\left(\frac{T}{N}\right)^2 \left[\frac{\sin\left(\frac{\omega T}{2}\right)}{(\omega - \omega_0)T/2} \right]^4 \left[\frac{1}{\frac{\omega}{\omega_0} + 1} \right]^4 \left[\sum_{n=1}^{N-1} \alpha_n \cos(nT\omega) \right]^2\right\} \quad (\text{E-25})$$

$$V(\omega) = \left(\frac{T}{N}\right)^2 \left[\frac{\sin \frac{\omega T}{2}}{(\omega - \omega_0)T/2} \right]^4 \left[\frac{1}{\frac{\omega}{\omega_0} + 1} \right]^4 \left\{ \left[\sum_{n=1}^{N-1} \gamma_n \cos(nT\omega) \right]^2 \right\} \quad (\text{E-26})$$

Expanding the last term in Equation (E-26)

$$\begin{aligned} \left\{ \left[\sum_{n=1}^{N-1} \gamma_n \cos(nT\omega) \right]^2 \right\} &= \left\{ \sum_{n=1}^{N-1} \gamma_n^2 \cos^2(nT\omega) + 2\gamma_1 \sum_{n=2}^{N-1} \gamma_n \cos(nT\omega) \right. \\ &\quad + 2\gamma_2 \sum_{n=3}^{N-1} \gamma_n \cos(nT\omega) \\ &\quad \left. + \dots + 2\gamma_{N-2} \gamma_{N-1} \cos[(N-1)T\omega] \right\} \quad (\text{E-27}) \end{aligned}$$

Looking at the first term in Equation (E-27)

$$\left\{ \sum_{n=1}^{N-1} \gamma_n^2 \cos^2(nT\omega) \right\} = \sum_{n=1}^{N-1} \left\{ \gamma_n^2 \right\} \cos^2(nT\omega) \quad (\text{E-28})$$

But, from Equation (E-18)

$$\left\{ \gamma_n^2 \right\} = \left\{ \left[\alpha_0 \alpha_n + \alpha_1 \alpha_{n+1} + \dots + \alpha_{N-1-n} \alpha_{N-1} \right]^2 \right\} \quad (\text{E-29})$$

$$\begin{aligned} &= \left\{ (\alpha_0 \alpha_n)^2 + (\alpha_1 \alpha_{n+1})^2 + \dots + (\alpha_{N-1-n} \alpha_{N-1})^2 \right. \\ &\quad \left. + 2\alpha_0 \alpha_n \left[\alpha_1 \alpha_{n+1} + \alpha_2 \alpha_{n+2} + \dots + \alpha_{N-1-n} \alpha_{N-1} \right] \right. \\ &\quad \left. + \dots + 2\alpha_{N-3-n} \alpha_{N-2-n} \alpha_{N-1-n} \alpha_{N-1} \right\} \quad (\text{E-30}) \end{aligned}$$

$$\mathcal{E}\left\{\gamma_n^2\right\} = (\alpha_0 \alpha_n)^2 + (\alpha_1 \alpha_{n+1})^2 + \dots + (\alpha_{N-1-n} \alpha_{N-1})^2 \quad (\text{E-31})$$

$$= N - n \quad (\text{E-32})$$

Thus,

$$\sum_{n=1}^{N-1} \mathcal{E}\left\{\gamma_n^2\right\} \cos^2(nT\omega) = \sum_{n=1}^{N-1} (N - n) \cos^2(nT\omega) \quad (\text{E-33})$$

The remaining terms in Equation (E-27) are of the form

$$\mathcal{E}\left\{2\gamma_j \sum_{n=j+1}^{N-1} \gamma_n \cos(nT\omega)\right\} \quad j < n$$

But

$$\mathcal{E}\left\{2\gamma_j \sum_{n=j+1}^{N-1} \gamma_n \cos(nT\omega)\right\} = 2 \sum_{n=j+1}^{N-1} \mathcal{E}\left\{\gamma_j \gamma_n\right\} \cos(nT\omega) \quad (\text{E-34})$$

$$= 0 \quad (\text{E-35})$$

Since

$$\mathcal{E}\left\{\gamma_j \gamma_n\right\} = 0 \quad (\text{E-36})$$

Thus the remaining terms in Equation (E-27) are identically zero.

Combining Equations (E-33) and (E-35), Equation (E-27) becomes

$$\mathcal{E}\left\{\left[\sum_{n=1}^{N-1} \gamma_n \cos(nT\omega)\right]^2\right\} = \sum_{n=1}^{N-1} (N - n) \cos^2(nT\omega) \quad (\text{E-37})$$

Substituting Equation (E-37) into Equation (E-26) gives the variance of the stochastic process $S_{NT}(\omega, \alpha_n)$.

$$V(\omega) = T^2 \left[\frac{\sin \frac{\omega T}{2}}{(\omega - \omega_0)T/2} \right]^4 \left[\frac{1}{\frac{\omega}{\omega_0} + 1} \right]^4 \sum_{n=1}^{N-1} \left(\frac{N-n}{N^2} \right) \cos^2(nT\omega) \quad (\text{E-38})$$

The variance is identically zero for $\omega = \omega_0 \pm K\left(\frac{2\pi}{T}\right)$, $K = 1, 2, 3, \dots$ and has a maximum value at $\omega = \omega_0$

$$\max \left\{ V(\omega) \right\} = \left(\frac{T}{4} \right)^2 \left[\frac{1}{2} - \frac{1}{N} \right]; \quad \omega = \omega_0 \quad (\text{E-39})$$

As the number of bits, N , becomes large

$$\lim_{N \rightarrow \infty} \left[\max \left\{ V(\omega) \right\} \right] = \frac{T^2}{32} \quad (\text{E-40})$$

The variance of the process $S_{NT}(\)$ as given in Equation (E-38) does not approach zero as N becomes large. To avoid that situation, a new estimate is defined.

Let

$$S_E(\omega) = \frac{1}{M} \sum_{i=1}^M S_i(\omega, \alpha_n) \quad (\text{E-41})$$

where $S_i(\omega, \alpha_n)$ is a particular realization of the process $S_{NT}(\omega, \alpha_n)$. That is, $S_i(\omega, \alpha_n)$ is a sample function from the ensemble represented by $S_{NT}(\omega, \alpha_n)$.

The expected value of $S_E(\omega)$ is

$$\mathcal{E}\{S_E(\omega)\} = \frac{1}{M} \sum_{i=1}^M \mathcal{E}\{S_i(\omega, \alpha_n)\} \quad (\text{E-42})$$

$$= \frac{T}{2} \left[\frac{\sin\left(\frac{\omega T}{2}\right)}{(\omega - \omega_0)T/2} \right]^2 \left[\frac{1}{\frac{\omega}{\omega_0} + 1} \right]^2 \quad (\text{E-43})$$

The variance of $S_E(\omega)$ is

$$V_E(\omega) = \frac{1}{M^2} \sum_{i=1}^M V_i(\omega) \quad (\text{E-44})$$

where $V_i(\omega)$ is the variance of $S_i(\omega, \alpha_n)$.

If the same number of bits are used for each $S_i(\omega, \alpha_n)$, then

$$V_1(\omega) = V_2(\omega) = \dots = V_M(\omega) = V(\omega) \quad (\text{E-45})$$

And Equation (E-44) becomes

$$V_E(\omega) = \frac{1}{M} V(\omega) \quad (\text{E-46})$$

$$= \frac{T^2}{M} \left[\frac{\sin\left(\frac{\omega T}{2}\right)}{(\omega - \omega_0)T/2} \right]^4 \left[\frac{1}{\frac{\omega}{\omega_0} + 1} \right]^4 \sum_{n=1}^{N-1} \left(\frac{N-n}{N^2}\right) \cos^2(nT\omega) \quad (\text{E-47})$$

Thus, the variance of the new estimate approaches zero as the number of sample functions, M , becomes large.

$$\lim_{M \rightarrow \infty} \left\{ V_E(\omega) \right\} = 0 \quad (\text{E-48})$$

For a given sample size M,

$$\max \left\{ V_E(\omega) \right\} = \left(\frac{T}{4} \right)^2 \left[\frac{1}{2} - \frac{1}{N} \right] \frac{1}{M}; \quad \omega = \omega_0 \quad (\text{E-49})$$

The estimate of the power spectrum as given by Equation (E-41) has the following two desirable characteristics

$$(1) \quad \mathcal{E} \left\{ S_E(\omega) \right\} = S(\omega) \quad (\text{E-50})$$

$$(2) \quad \lim_{M \rightarrow \infty} \left\{ V_E(\omega) \right\} = 0 \quad (\text{E-51})$$

Therefore, $S_E(\omega)$ is an unbiased estimate of $S(\omega)$ with arbitrarily small variance, and is obtained by arithmetically averaging M different spectra of randomly generated, equal code length, biphasic modulated sinusoids.

APPENDIX F

S/C POWER RATIO TABLES

The combined effects of the TM modulation index, TM bit rate, and subcarrier filter bandwidth as given in Equation (B-69) have been summarized in matrix form in Table F-1. Each entry in the matrix represents a unique combination of bit rate, modulation index, and bandwidth. (The range of values for the parameters were chosen to include those values presently used by NASA.)

Table F-1. Spur-to-Carrier Ratios (in dB) for Various Combinations of TM Modulation Index and Bit Period - Bandwidth Product*

Bit Period - Bandwidth Product ($T\Omega$)

	13.0	13.5	14.0	14.5	15.0	15.5	16.0	16.5	17.0	17.5	18.0
0.1	-65.4	-65.6	-65.8	-66.2	-66.6	-67.1	-67.6	-68.3	-69.0	-69.7	-70.5
0.2	-53.3	-53.5	-53.7	-54.1	-54.5	-55.0	-55.5	-56.2	-56.9	-57.6	-58.4
0.3	-46.2	-46.4	-46.6	-46.9	-47.4	-47.9	-48.4	-49.1	-49.8	-50.5	-51.3
0.4	-41.1	-41.2	-41.5	-41.8	-42.2	-42.7	-43.3	-43.9	-44.6	-45.4	-46.1
0.5	-37.1	-37.2	-37.4	-37.8	-38.2	-38.7	-39.3	-39.9	-40.6	-41.3	-42.1
0.6	-33.7	-33.8	-34.1	-34.4	-34.8	-35.3	-35.9	-36.5	-37.2	-38.0	-38.7
0.7	-30.8	-30.9	-31.2	-31.5	-31.9	-32.4	-33.0	-33.6	-34.3	-35.0	-35.8
0.8	-28.2	-28.3	-28.6	-28.9	-29.3	-29.8	-30.4	-31.0	-31.7	-32.4	-33.2
0.9	-25.8	-25.9	-26.2	-26.5	-26.9	-27.4	-28.0	-28.6	-29.3	-30.0	-30.8
1.0	-23.6	-23.7	-23.9	-24.3	-24.7	-25.2	-25.8	-26.4	-27.1	-27.8	-28.6
1.1	-21.5	-21.6	-21.8	-22.2	-22.6	-23.1	-23.6	-24.3	-24.9	-25.7	-26.4
1.2	-19.4	-19.6	-19.8	-20.1	-20.5	-21.0	-21.6	-22.2	-22.9	-23.6	-24.4
1.3	-17.4	-17.6	-17.8	-18.1	-18.5	-19.0	-19.6	-20.2	-20.9	-21.6	-22.4
1.4	-15.4	-15.5	-15.8	-16.1	-16.5	-17.0	-17.6	-18.2	-18.9	-19.6	-20.3
1.5	-13.4	-13.5	-13.7	-14.1	-14.5	-15.0	-15.5	-16.1	-16.8	-17.5	-18.2

*The first spur ($k = 1$)

Table F-1. Spur-to-Carrier Ratios (in dB) for Various Combinations of
 TM Modulation Index and Bit Period - Bandwidth Product (Continued)

Bit Period - Bandwidth Product ($T\Omega$)

	18.5	19.0	19.5	20.0	20.5	21.0	21.5	22.0	22.5	23.0	23.5
0.1	-71.3	-72.1	-72.9	-73.6	-74.3	-74.9	-75.4	-75.8	-76.1	-76.3	-76.4
0.2	-59.2	-60.0	-60.8	-61.5	-62.2	-62.8	-63.3	-63.7	-64.0	-64.2	-64.3
0.3	-52.1	-52.8	-53.6	-54.4	-55.0	-55.6	-56.1	-56.5	-56.9	-57.1	-57.2
0.4	-46.9	-47.7	-48.5	-49.2	-49.9	-50.5	-51.0	-51.4	-51.7	-51.9	-52.1
0.5	-42.9	-43.7	-44.5	-45.2	-45.9	-46.5	-47.0	-47.4	-47.7	-47.9	-48.0
0.6	-39.5	-40.3	-41.1	-41.8	-42.5	-43.1	-43.6	-44.0	-44.3	-44.5	-44.6
0.7	-36.6	-37.4	-38.2	-38.9	-39.6	-40.2	-40.7	-41.1	-41.4	-41.6	-41.7
0.8	-34.0	-34.8	-35.5	-36.3	-36.9	-37.5	-38.0	-38.4	-38.8	-39.0	-39.1
0.9	-31.6	-32.4	-33.1	-33.9	-34.5	-35.1	-35.6	-36.0	-36.3	-36.6	-36.7
1.0	-29.3	-30.1	-30.9	-31.6	-32.3	-32.9	-33.4	-33.8	-34.1	-34.3	-34.4
1.1	-27.2	-28.0	-28.8	-29.5	-30.2	-30.8	-31.3	-31.7	-32.0	-32.2	-32.3
1.2	-25.2	-25.9	-26.7	-27.4	-28.1	-28.7	-29.2	-29.6	-29.9	-30.1	-30.2
1.3	-23.1	-23.9	-24.7	-25.4	-26.0	-26.6	-27.1	-27.5	-27.8	-28.0	-28.2
1.4	-21.1	-21.9	-22.6	-23.3	-24.0	-24.6	-25.1	-25.5	-25.8	-26.0	-26.1
1.5	-19.0	-19.8	-20.5	-21.2	-21.9	-22.5	-23.0	-23.4	-23.7	-23.9	-24.0

*The first spur ($k = 1$)

Table F-1. Spur-to-Carrier Ratios (in dB) for Various Combinations of
TM Modulation Index and Bit Period - Bandwidth Product* (Continued)

Bit Period - Bandwidth Product ($T\Omega$)

	24.0	24.5	25.0	25.5	26.0	26.5	27.0	27.5	28.0
0.1	-76.5	-76.5	-76.5	-76.5	-76.5	-76.6	-76.6	-76.7	-76.9
0.2	-64.4	-64.4	-64.4	-64.4	-64.4	-64.5	-64.5	-64.7	-64.8
0.3	-57.3	-57.3	-57.3	-57.3	-57.3	-57.3	-57.4	-57.5	-57.7
0.4	-52.1	-52.2	-52.2	-52.2	-52.2	-52.2	-52.3	-52.4	-52.5
0.5	-48.1	-48.1	-48.1	-48.1	-48.1	-48.2	-48.2	-48.3	-48.5
0.6	-44.7	-44.7	-44.8	-44.8	-44.8	-44.8	-44.9	-45.0	-45.1
0.7	-41.8	-41.8	-41.8	-41.8	-41.8	-41.9	-41.9	-42.0	-42.2
0.8	-39.2	-39.2	-39.2	-39.2	-39.2	-39.2	-39.3	-39.4	-39.6
0.9	-36.8	-36.8	-36.8	-36.8	-36.8	-36.8	-36.9	-37.0	-37.2
1.0	-34.5	-34.5	-34.5	-34.5	-34.6	-34.6	-34.7	-34.8	-34.9
1.1	-32.4	-32.4	-32.4	-32.4	-32.4	-32.4	-32.5	-32.6	-32.8
1.2	-30.3	-30.3	-30.3	-30.3	-30.3	-30.4	-30.4	-30.5	-30.7
1.3	-28.2	-28.3	-28.3	-28.3	-28.3	-28.3	-28.4	-28.5	-28.6
1.4	-26.2	-26.2	-26.2	-26.2	-26.2	-26.3	-26.3	-26.4	-26.6
1.5	-24.1	-24.1	-24.1	-24.1	-24.1	-24.1	-24.2	-24.3	-24.4

*The first spur ($k = 1$)